Archives of Civil and Mechanical Engineering (2025) 25:74
https://doi.org/10.1007/s43452-025-01128-3

ORIGINAL ARTICLE

Impact of attapulgite and basalt fiber additions on the performance of pumice-based foam concrete: mechanical, thermal, and durability properties

Burak Bodur[1] · Ahmet Benli[2] · Oguzhan Yavuz Bayraktar[3] · Haluk Görkem Alcan[4] · Gokhan Kaplan[5] · Abdulkadir Cüneyt Aydın[5]

Received: 18 September 2024 / Revised: 30 November 2024 / Accepted: 8 January 2025 / Published online: 29 January 2025

Abstract

This study explored the combined effects of using attapulgite (ATP) as a partial cement replacement and basalt fibers (BF) as reinforcement in the development of high-performance foam concrete (FC) with 100% pumice aggregate. The experimental program included preparing FC mixtures with ATP replacements at 10%, 20%, and 30% by cement weight, and adding BF at volume fractions of 0.5%, 1.0%, and 2.0%. Key properties assessed were fresh flowability, compressive and flexural strengths, stress–strain behavior, thermal conductivity, and durability under sulfate exposure and high temperatures. Findings revealed a synergistic effect between ATP and BF, leading to significant performance enhancements across various parameters. The mixture with 30% ATP and 0.5% BF exhibited the highest compressive strength, reaching 19.45 MPa at 28 days and 22.11 MPa at 90 days, indicating improvements of 129.3% and 85.3% over the reference mix, respectively. This combination also achieved the lowest sorptivity, improved thermal stability, and better sulfate resistance, making it highly suitable for structural applications in harsh environments. In addition, the mixture with 10% ATP and 0.5% BF demonstrated the lowest thermal conductivity, reducing heat transfer by 4.2% compared to the control, which is beneficial for thermal insulation in building materials. Microstructural analysis using Scanning Electron Microscopy (SEM) showed that ATP's pozzolanic reactivity led to a denser microstructure with stronger bonding, while BF effectively bridged micro-cracks, enhancing the FC matrix's durability. Overall, these results highlighted the potential of ATP and BF to significantly enhance FC's mechanical, thermal, and durability properties, providing an eco-friendly solution with lower cement use and greater resilience to environmental stressors. This study contributes to sustainable construction technology by showcasing how ATP and BF can optimize FC performance, supporting its wider use in the construction industry.

Keywords Basalt fiber-reinforced foam concrete · Pumice · Attapulgite · Stress–strain · Strength · Durability

1 Introduction

The building sector has seen a rise in the use of foam concrete (FC) during the last few decades [1]. Better workability, reduced weight, improved thermal performance, increased fire resistance, and lower cost are some of the advantages of FC over traditional concrete [2]. A creative and effective construction technique called FC has been successfully used in a number of Asian and European nations [3]. Alternatively, FC falls into the category of low density concrete, cellular concrete, or aircrete, with densities ranging from 300 to 1800 kg/m^3. Its exceptional flowability [4], low self-weight [5], minimal aggregate consumption [6], high porosity [7], fire resistance [8], excellent heat insulation, airborne sound insulation, and required compressive

✉ Ahmet Benli
abenli@bingol.edu.tr

[1] Project and Technology Office, Bartın University, Bartın 74100, Turkey

[2] Civil Engineering Department, Bingol University, Bingol 12100, Turkey

[3] Civil Engineering Department, Kastamonu University, Kastamonu 37150, Turkey

[4] Civil Engineering Department, Kafkas University, Kars 36100, Turkey

[5] Civil Engineering Department, Atatürk University, Erzurum 25030, Turkey

strength are only a few of its unique characteristics. The primary components of this lightweight concrete are cement, filler, foam, and water [9]. Unlike regular concrete, FC mixes do not include coarse materials. This kind of concrete can be utilized for a number of projects, such as road embankments, floor insulation [10], soft ground areas, backfilling retaining walls [11], and slope filling [12]. Although porous concrete has traditionally been made with air-entraining agents or lightweight aggregates [13], fresh cement paste or mortar is typically combined with manufactured foam, such as a foaming agent, to generate FC [14]. FC had a higher porosity and a lower density, but the increased porosity also contributed to its reduced strength. This made it challenging to employ FC in certain circumstances where a significant degree of strength was necessary. Due of FC's drawback, many attempts have been undertaken to obtain both high strength and low density [15]. Using lightweight aggregates can contribute to obtain lower density and further reduce the heat conductivity of FC and one possible substitute for fine aggregate is pumice aggregate (PA) [16]. Pumice, which is naturally occurring and has a structure akin to a sponge, is formed when molten lava cools quickly and forms granules. In certain countries, such as US, Italy, Greece, Turkey, and Spain, it is utilized as an aggregate in the creation of lightweight concrete [17]. Pumice has been particularly used as an aggregate in concrete to produce lightweight concrete [18]. A practical method for creating lightweight, workable, affordable [19], and ecologically friendly concrete is the addition of pumice as an aggregate [20]. The application of fine and coarse PA in cement-based concrete was examined by Gündüz and Uğur [21], who found that the strength of lightweight concrete including PA was comparable to that of standard weight concrete. Jamal et al. [18] investigated PA incorporated geopolymer concrete. The authors reported that the thermal conductivity and oven dry density were found to be between 0.119 and 0.131 W/m K and 1746 and 1815 kg/m^3, respectively.

The total cost of production could go up if FC uses more cement. Thus, it is preferable to have the option of using supplemental cementitious materials (SCMs), particularly in larger volumes, to lower the amount of cement used and the 8% global carbon emissions that OPC contributes to [22]. Attapulgite (ATP), often referred to as palygorskite mineral, is a magnesium aluminum silicate clay that has attracted a lot of interest from several study sectors due to a number of its properties, including its large surface area, interlayer enormous void-texture, and comparatively low cost [23]. These benefits allow ATP to be utilized in FC blends as a cement alternative. Certain studies suggest that ATP can be used as SCMs to reduce the amount of cement clinker consumed. The addition of high-reactivity ATP in conjunction with an increase in the curing temperature, for example, has been shown in studies by Zghair et al. [24] to enhance the compressive strength of cement slurry at later ages. Additionally, Kawashima et al. [25] examined the impact of a tiny quantity of high-purity ATP on the adhesive characteristics of cement slurry and discovered that ATP increased the slurry's cohesion and viscosity.

Many disadvantages affect FC, including excessive porosity, brittleness, low ductility, significant drying shrinkage, and poor resistance to breaking and deformation. To increase FC's tensile strength and fracture resistance, engineers usually utilize fibers, such as steel fibers [26], polymer fibers [27], and basalt fibers [28] as the recommended reinforcement material [29]. Basalt fibers (BF) is becoming more and more popular as a substitute for other fibers like carbon fibers because of its enhanced qualities and sustainable production, while the manufacture of BF is comparable to that of glass fiber, and its low energy consumption and lack of chemicals in the process make it more environmentally friendly [30]. Even though BF is widely used in applications, including fire protection automotive parts, sports equipment, and electrical insulation, more research is needed on its use in cement-based materials [31]. When BF is added to concrete, it gets stronger and shrinks less [32]. Wang et al. [33] investigated the combination of basalt and sisal fibers to increase the durability and mechanical characteristics of lightweight roadbed FC. The authors reported that FC made with a blend of 0.2% sisal and 0.1% BF had greater compressive and flexural strengths, with improvements of 18.04% and 52.44%, respectively. Shi et al. [28] examined the impacts of re-dispersible latex powder and BF on the FC's microstructure, water adsorption rate, compressive strength, and dry and wet densities. The density and the rate of water adsorption were shown to be marginally impacted by BF.

The objective of this paper was to enhance sustainable construction materials by investigating the combined use of ATP and BF in FC made entirely from pumice aggregate. This study addressed several ongoing challenges in foam concrete, including the need to improve strength, thermal insulation, and durability under various environmental stressors. By utilizing ATP as a partial replacement for cement, the research explored the potential for reducing cement consumption and, consequently, lowering the carbon footprint of FC while harnessing ATP's pozzolanic properties to fortify the concrete matrix. The incorporation of basalt fibers, recognized for their reinforcing capabilities, aimed to enhance FC's resistance to cracking, brittleness, and deformation-key issues that hindered the broader application of FC in load-bearing and high-performance scenarios. The research encompassed a thorough series of experiments to evaluate the effects of varying proportions of ATP and BF on both the fresh and hardened properties of FC. Specifically, it examined parameters, such as fresh flowability, compressive and flexural strengths, stress–strain behavior, thermal conductivity, and durability in the face of sulfate exposure and elevated temperatures. This methodology facilitated a detailed understanding of how ATP and BF contributed individually and synergistically to the enhancement of FC's structural and functional characteristics. Furthermore, the study employed microstructural analysis using Scanning Electron Microscopy (SEM) to investigate the changes in internal bonding and pore structure resulting from ATP's pozzolanic reactivity and BF's fiber-bridging effect. By elucidating these impacts, the research aimed to present a high-performance, eco-friendly variant of FC with improved resistance to harsh environmental conditions, making it suitable for structural applications, particularly in regions that demanded lightweight, durable, and thermally efficient building materials. Ultimately, this research contributed to the advancement of sustainable construction materials by demonstrating how ATP and BF could be effectively utilized to optimize FC, providing a practical solution for reducing cement demand, enhancing resilience, and expanding the application of FC in the construction industry, especially in challenging environments.

1.1 Research significance

This study investigated advancements in sustainable construction materials by analyzing the effects of ATP and BF on FC composed entirely of pumice aggregate. Although FC was valued for its lightweight and insulating properties, its mechanical strength and brittleness posed limitations for structural applications. The research incorporated ATP as a partial cement replacement and added BF as reinforcement to improve the mechanical, thermal, and durability characteristics of FC. ATP, a cost-effective clay mineral, reduced the cement content in FC mixes, resulting in a lower carbon footprint. Its pozzolanic properties were anticipated to enhance the density and bonding of the cementitious matrix, thereby improving compressive strength and resilience against environmental stressors, such as high temperatures and sulfate exposure, in line with sustainability goals. BF notably strengthened the structural integrity of FC by increasing tensile strength, decreasing brittleness, and providing resistance to cracking and deformation. Additionally, BF's eco-friendly production processes were consistent with green construction objectives. The study assessed various properties of FC, including flowability, compressive strength, and thermal conductivity. Microstructural analysis using Scanning Electron Microscopy (SEM) illustrated how ATP and BF improved internal bonding and pore structure. Overall, the findings highlighted the potential of ATP and BF to develop a robust, eco-friendly alternative for structural applications, thereby fostering more sustainable construction practices.

2 Experimental program

2.1 Starting materials

According to EN 197-1 standard, CEM I 42.5R cement was the principal binder employed in this investigation. The cement utilized has a specific gravity of 3.13 and a specific surface area of 3300 cm^2/g (Blaine fineness). This study used attapulgite, a clay-based aluminosilicate precursor material, instead of cement. Attapulgite has a specific gravity of 1.35. The chemical composition of attapulgite and cement is presented in Table 1. Figure 1 depicts the XRD pattern of the mineral attapulgite. The XRD pattern showed that the attapulgite had peaks of dolomite, quartz, and attapulgite. The cement and attapulgite particle sizes are distributed as seen in Fig. 2. The average particle size of cement and attapulgite is 21.9 and 23.3 µm, respectively. The grain size distributions of these two powders are close to each other.

Pumice aggregate (PA) with a sieve opening of 0–4 mm was used to prepare the mixtures. Pumice aggregate's saturated dry surface density is 1.23 g/cm^3, and water absorption is 29.9%. The grain size distributions of the pumice aggregate are displayed in Fig. 3, following the ASTM C33 [34] standard. Because pumice aggregate absorbs a lot of water, a new generation superplasticizer based on polycarboxylic ether (PCE) was added to the blends to make the mixes more flowable. PCE has a specific gravity of 1.06 ± 2, with 32% solids by weight. A foaming agent based on an organic resin was used to prepare the mixtures further to reduce the fresh and hardened unit weight. Basalt fibers (BF) of 12 mm length produced foam concrete. The technical specifications of the BF are demonstrated in Table 2.

2.2 Mixing procedure and preparation of the specimens

A cement quantity of 500 kg/m^3 was used to produce the test specimens. Instead of cement, 10, 20, and 30% attapulgite was used. The water/binder (cement + attapulgite) ratio of all mixtures was 0.25. BF was added to the mixtures at 0.5,

Table 1 Chemical composition (by weight) of attapulgite and cement

Oxide (%)	CaO	SiO_2	Al_2O_3	Fe_2O_3	MgO	Na_2O	K_2O	SO_3	LOI
Cement	63.8	21.6	4.5	5.6	1.5	0.2	0.3	1.8	0.6
Attapulgite	8.8	65.7	12.3	4.7	5.2	0.9	1.8	0.3	0.2

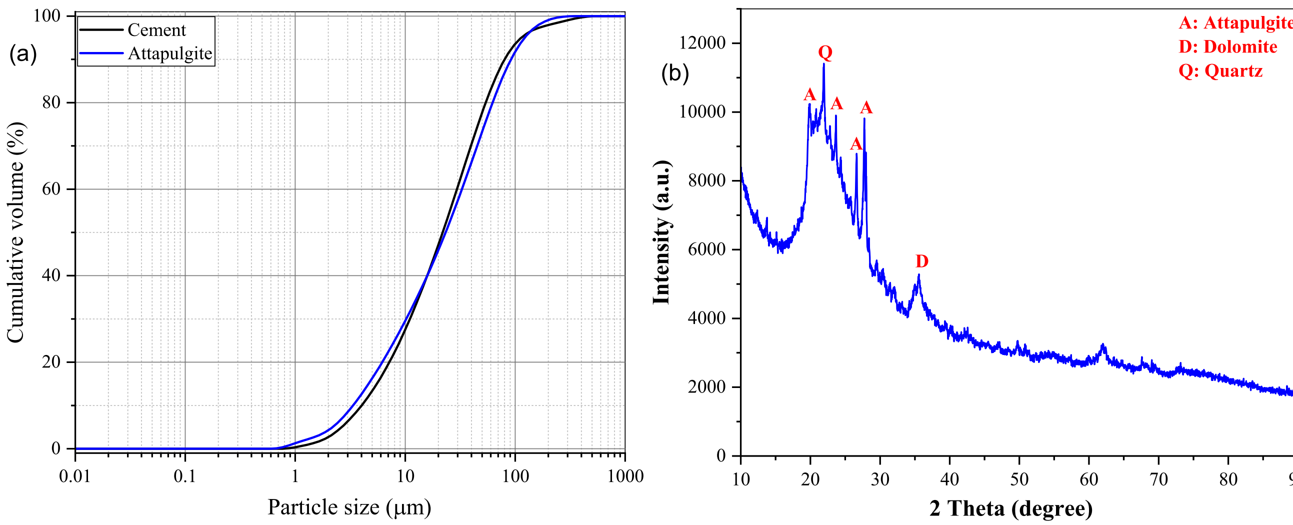

Fig. 1 **a** Grain size distributions of cement and ATP, and **b** XRD pattern of ATP

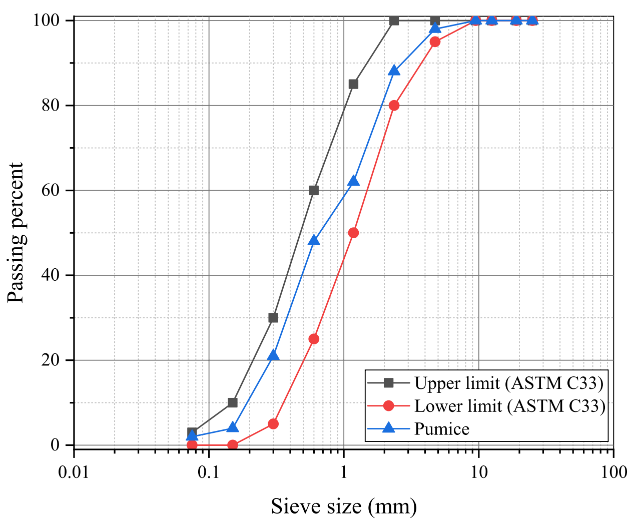

Fig. 2 Grain size distributions of pumice aggregate

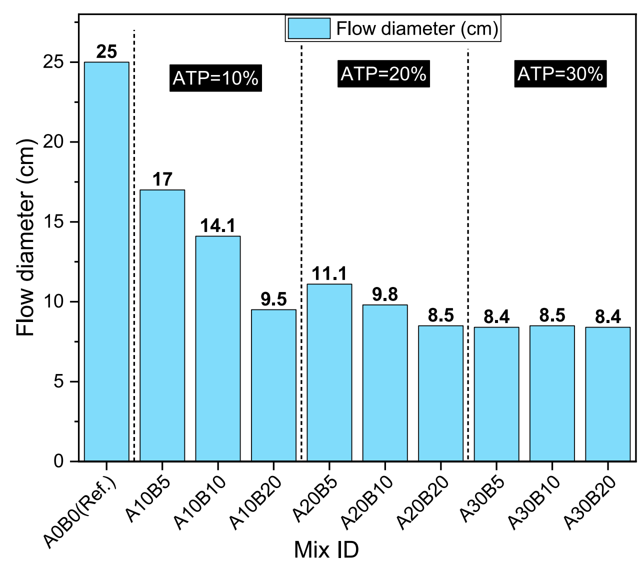

Fig. 3 Flow diameters of FC mixtures

1 and 2% by volume. As a result of the preliminary tests, it was determined that the optimum foam volume is 480 kg/m^3. When preparing the foam, the foaming agent was used in an amount of 3% of the weight of the water. In other words, 30 g of foaming agent were used for 1 L of water. The foam obtained with a high-speed mixer was added to the mixture. The first step involved mixing two-thirds of the water with the cement (or attapulgite, if it was available) for 1 min at a moderate speed and another minute at a high speed. After that, the mixture was combined with the remaining water and PCE, and it was mixed quickly for 2 min. The third step involved adding pumice to the freshly combined slurry and mixing it for 1 min at a moderate speed and another minute at a fast speed. Following the addition of the foam, the mixture was stirred for 2 min at a low pace. BF was added to the mixture in the final phase, and it was mixed for 1 min at a moderate speed and 2 min at a high speed. The prepared fresh mixture was placed in molds. The surface of all molds was covered with cling film. The samples were stored for 24 h under laboratory conditions. The demolded specimens were cured in water until the test day. The mixing ratios and

Table 2 Technical specifications of the BF

Length	Diameter	Density	Elastic modulus	Elongation at break	Color
12 mm	13 μm	2.65 g/cm^3	90 GPa	~%3	Golden brown

material quantities of the samples produced in this study are listed in Table 3.

2.3 Experimental method

The flow diameters of the fresh mixtures were determined based on ASTM C1437 [35] standard. According to ASTM C642 [36], measurements of characteristics, such as oven dry density, apparent porosity, and water absorption, were made. These experiments were determined after 90 days of curing. To determine the physical properties, 50 × 50 × 50 mm cube samples were produced. After 28 and 90 days, the mechanical characteristics of the foam concrete specimens, including their compressive and flexural strengths, were ascertained. The three-point flexural strength was determined on the 28th and 90th day on 40 × 40 × 160 mm specimens as per ASTM C348 [37]. ASTM C349 [38] standard measured the compressive strength of the specimens broken during this test. 100 × 200 mm-sized cylinder specimens were used to determine the stress–strain curves of foam concretes. In this context, ASTM C469 [39] standard is taken as basis. Stress–strain curves of all specimens were drawn after 28 and 90 days and these curves were also obtained after durability tests.

Foam concretes were exposed to high temperature at 200, 400, and 600 °C after 28 days curing period. To determine the specimens' weight loss and compressive strength, 50 × 50 × 50 mm specimens were produced. After reaching the target temperature, the samples were exposed to this temperature for 2 h. Afterward, the samples were allowed to cool down (slow cooling) in the furnace. A muffle furnace with a heating rate of 5 °C/min was used for these tests.

In addition, 5% $MgSO_4$ solution was prepared to determine the sulfate resistance of foam concretes. The specimens were exposed to this solution for 90 days. Every 15-day period, the solution was updated. On the 90th day, weight loss and compressive strength of 50 × 50 × 50 mm cube specimens were measured. After 90 days of curing, the thermal conductivity of the specimens was determined according to ASTM C518 [40] standard. The thermal conductivity coefficients of the samples were measured after drying at 50 °C for 3 days. For this test, 200 × 200 × 30 mm-sized plaque specimens were produced. Sorptivity was determined to assess the permeability properties of the samples. ASTM C1585 [41] standard was used for this test and 50 × 50 × 50 mm cube specimens were produced. Sorptivity of the specimens was also determined after 90 days of curing.

FC sample microstructure analyses were done at the MERLAB unit at Munzur University. For microstructure studies, SEM pictures were acquired at various magnifications. For this, Quanta FEG 250 model device was utilized. Microstructural analyses were performed on specimens that had cured for 28 days and mixes that had been exposed to high temperatures and sulfate attack (Table 4).

3 Results and discussion

3.1 Fresh characteristics of FC mixtures

The effect of ATP as a cement substitute and the amount of BF on the fresh properties of FC mixtures, including 100% PA, is shown in Fig. 3 in terms of flow diameter results. As the percentages of ATP and BF increase, the mixes' flow diameters, which range from 25 to 8.4 cm and are clearly shown to decrease in Fig. 3. The water/cement ratio was maintained at 0.25 throughout the sample preparation procedure to evaluate the impacts of BF and ATP in FC mixes. It was discovered that the high water absorption capacity of ATP, which may reach up to 180% of its mass, decreased the workability of FC mixes [43] was substituted for cement and BF was added, as depicted in Fig. 3. When ATP was substituted for PC in FC mixes, the flow diameter decreased [44], and with a rise in ATP content, this decline intensified [45]. The enormous specific surface area, water-absorption capacity, and nonporous structure of ATP, which reduces flow diameters, all contribute to its explanation [46]. Moreover, the fine-grained ATP-induced

Table 3 Mixing ratios and material quantities (kg/m^3)

Mix ID	BF (%)	ATP (%)	Cement	ATP	Water	PCE	PA	Foam	BF
A0B0 (Ref.)	0	0	500.0	0.0	125.0	15.0	377.4	96.0	0.0
A10B5	0.5	10	450.0	50.0	125.0	15.0	331.5	96.0	13.3
A10B10	1.0	10	450.0	50.0	125.0	15.0	323.0	96.0	26.5
A10B20	2.0	10	450.0	50.0	125.0	15.0	306.0	96.0	53.0
A20B5	0.5	20	400.0	100.0	125.0	15.0	294.1	96.0	13.3
A20B10	1.0	20	400.0	100.0	125.0	15.0	285.6	96.0	26.5
A20B20	2.0	20	400.0	100.0	125.0	15.0	268.6	96.0	53.0
A30B5	0.5	30	350.0	150.0	125.0	15.0	256.6	96.0	13.3
A30B10	1.0	30	350.0	150.0	125.0	15.0	248.1	96.0	26.5
A30B20	2.0	30	350.0	150.0	125.0	15.0	231.1	96.0	53.0

Table 4 Lists the summary of test methods, standards, testing time, and sample sizes

Test	Test time	Sample size (mm)	Standard
Flow diameter	Fresh mortar	–	ASTM C1437 [35]
Physical properties	90th day	50 × 50 × 50	ASTM C642 [36]
Flexural strength	28th and 90th day	40 × 40 × 160	ASTM C348 [37]
Compressive strength	28th and 90th day	Specimen broken in flexural test	ASTM C349 [38]
Stress–strain		100 × 200 mm cylinder	ASTM C469 [39]
Sorptivity	90th day	50 × 50 × 50	ASTM C1585 [41]
Thermal conductivity	90th day	200 × 200 × 30	ASTM C518 [40]
High temperature	200–400–600 °C	50 × 50 × 50	–
$MgSO_4$ attack	Up to day 90 days	50 × 50 × 50	ASTM C1012 [42]

increase in the aggregate surface of FC mixes led to a decrease in the flow diameters. The lowest workability value of 8.4 cm which is lower than the reference mixture by about 66.4% was achieved when cement was replaced with 30%ATP and with 0.5 and 2%BF included, and the reference mixture with 0%ATP and 0%BF had the largest flow diameter, measuring 25 cm. BF addition also resulted in a decrease in the flow diameters of FC combinations, as can be seen clearly in Fig. 3. This is largely because of the BF's increased friction force [47] and improved cohesiveness with the matrix, which both reduce mixture fluidity [48]. FC mixes were shown to become less workable and more viscous when fibers were added. This observation suggests that the fibers may hinder the aggregates' free mobility. The flow diameters of 10%ATP-incorporated mixtures reduced to 17, 14.1, and 9.5 cm at 0.5, 1, and 2%BF content leading to flowability reduction of 47, 43.6, and 62%, respectively, compared to the reference mixture. Similar reduction in flowability was clearly seen as illustrated in Figs. 3 and 5 when 20 and 30%ATP were substituted for cement. For mixes containing 20% ATP, the flow diameters decreased to 11.1, 9.8, and 8.5 cm at 0.5, 1%, and 2% BF content, respectively, resulting in a reduction in flowability of 55.6, 60.8, and 66% as per the reference mixture. The flow diameters for mixes with 30% ATP dropped to 8.4, 8.5, and 8.4 cm at 0.5, 1%, and 2% BF concentration, respectively. This meant that the mixes' flowability was reduced by 55.6, 60.8, and 66% in comparison to the reference mixture. The reduced workability of the mixtures with 30% ATP and BF was attributed to ATP's high water absorption and the increased internal friction from the fibers, which restricted particle movement and significantly decreased the flow diameter compared to the reference mixture.

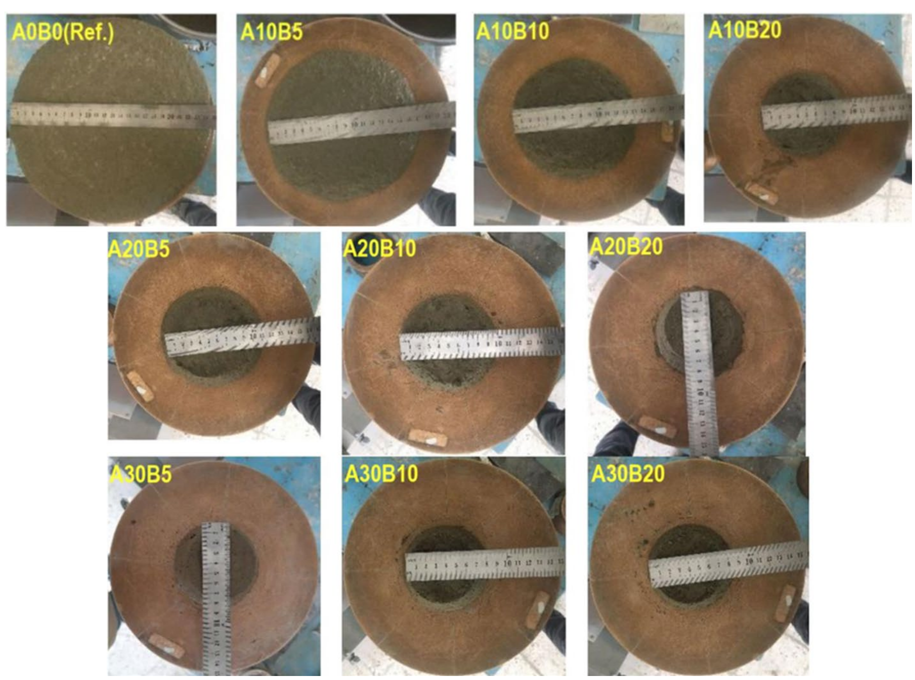

Fig. 4 The slump flow measurements for various FC mixtures

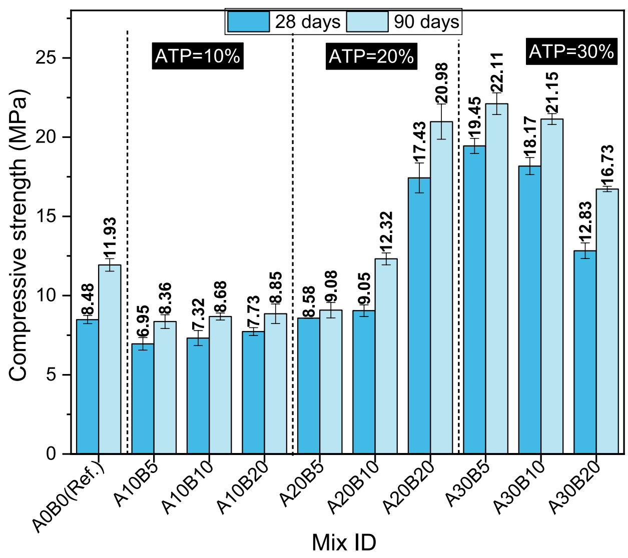

Fig. 5. 28- and 90-Day compressive strength of FC mixtures

Figure 4 displays the images obtained from the flow diameter tests that were conducted to evaluate the FC blends' flowability characteristics.

3.2 Compressive strength

Figure 5 depicts the impact of BF content and ATP as a cement substitute on the 28- and 90-day compressive strengths of FC mixes containing 100% pumice aggregate (PA). Figure 5 illustrates the strength improve that was seen as the curing age increased. The specimens of FC mixtures with 10%ATP showed a compressive strength that varied from 6.95 to 7.73 MPa and from 8.36 to 8.85 MPa at 28 days and 90 days, respectively. As shown in Fig. 5, during both curing ages, the FC combinations' compressive strength was lower than the reference mixture when cement was replaced with 10% ATP. Strength reductions with the addition of 10%ATP as compared to the reference blend were in the range of 8.84 and 18% at 28 days, and 25.81 and 29.92% at 90 days, showing more strength loss at later ages. On the other hand, adding BF reduced the compressive strength loss of 10% ATP-incorporated mixes as BF content increased. Since the addition of BF enhanced the compressive strength, the mixes incorporating 10% ATP and 2% BF at both curing ages attained the highest strength. Numerous research have reported that the reason for these improvement in compressive strength is because BF occupy the pores of the concrete in different orientations, improving the strength of the material [49]. Because of their small sizes, BF can lower the stress concentrations that cause micro-cracks to propagate farther in concrete [50], improve the cracking resistance and ductility of the material, and generally enhance concrete performance [51]. Niaki et al. [52] reported that adding BF at a dosage of 0.5–3.5 wt% enhanced the compressive strength to an ideal fiber content of 2%. At a 2% fiber dosage, the compressive strength rose by almost 10% when compared to the control mix. Nevertheless, the compressive strength decreased by roughly 12% and 21%, respectively, upon the additional increase in BF dosage to 2.5% and 3%.

When 20% ATP-incorporated FC mixtures were considered, all mixtures exhibited higher strength enhancement as compared the mixtures with 10%ATP but only the mixture with 0.5%BF had a slight lower strength at 90 days than the reference blend. The other two 20% ATP-incorporated mixtures containing 1 and 2%BF attained higher strength than the reference blend. The compressive strength enhanced significantly and increased to 17.43 and 20.98 MPa at 28 and 90 days for the blend comprising 20%ATP and 2%BF(A20B20). The enhancements in the strength for this mixture were 105.54 and 75.85% as per the reference mixture. The American Concrete Institute standard (ACI 318) [53] states that concrete is adequate for structural purposes if, after 28 days of curing, its compressive strength values are equal to or greater than ~ 17 MPa. The FC mix containing 20%ATP and 2%BF were suitable for structural purposes, because it had compressive strength greater than 17 MPa. The mixture with 20%ATP that performed the best in terms of compressive strength was the one that combined 20%ATP and 2%BF.

When FC mixes containing 30% ATP were taken into account, all of the mixtures showed greater strength enhancement when compared to the reference blend, the mixes comprising 10% ATP and the 20%ATP-incorporated mixtures with 0.5 and 1%BF. The A30B5 mixture, comprising 30% ATP and 0.5% BF, achieved the highest compressive strength, showing remarkable gains of 129.3% at 28 days and 85.33% at 90 days compared to the reference mix. This enhanced performance results from the synergistic effects of ATP's pozzolanic reactivity combined with the optimal reinforcement level of BF, which together strengthen the FC matrix. The FC mixes containing 30%ATP and 1%BF were also suitable for structural purposes, because they had compressive strength greater than 17 MPa. At 30%ATP content, increase in BF content decreased the compressive strength slightly at 1%BF and more decrease was measured at 2% BF. The rise in compressive strength was verified by the thermos-gravimetric study's data, which also demonstrated that ATP shows increased the pozzolanic reactivity at later ages after 28 days [43]. ATP functioned as a pozzolanic material, reacting with calcium hydroxide generated during cement hydration to produce additional calcium silicate hydrate (C–S–H) gel. This secondary C–S–H formation led to a denser, more robust matrix by filling micro-pores and enhancing the overall cohesion and strength of the FC. The pozzolanic reaction of ATP was especially effective at later ages (beyond 28 days), accounting for the continued strength gains observed at 90 days. The addition of 0.5% BF offered effective crack-bridging and reinforcement while preserving the concrete matrix's homogeneity. Basalt fibers enhanced the tensile and compressive properties of FC by inhibiting crack propagation and improving load distribution within the matrix [54]. At this optimal fiber content, the fibers were evenly dispersed, maintaining good workability and efficiently bridging cracks, which led to an increase in compressive strength [55]. Utilizing 30% ATP and 0.5% BF created a balance between the matrix densification provided by ATP and the crack resistance offered by BF. This equilibrium was crucial, as ATP strengthened the matrix through additional C–S–H formation, while BF reinforced it without the risk of excessive fiber content, which could lead to clustering, voids, or decreased workability. Increasing the fiber content would have upset this balance, while reducing the amount of ATP would have lessened pozzolanic reactivity and matrix densification.

3.3 Stress–strain curves after 28 and 90 days curing

Figure 6 depicts the impact of BF content and ATP as a cement substitute on the 28- and 90-day axial stress–strain behavior of FC mixes. Stress enhancement was noticed with an increase in curing age, as shown in Fig. 6, but strain was generally reduced with the increase in curing age. Peak stress values were the same as the compressive strength values illustrated in Fig. 5. Observations reveal that the reference combination containing 0%ATP and 0% BF reached the peak strength then it failed without no much strain, a brittle failure occurred. However, the mixtures with BF exhibited strength loss gradually with increasing strain after peak stress. When the content of ATP decrease in FC mixtures, the specimens demonstrated the ability to support load at increasing strains once the compressive peak strength was attained. As a result of the fiber reinforcement creating connection bridges on the concrete, it stopped cracks from growing, which was the behavior that was linked to the specimens' increased integrity. More strains were reported after peak strains with the increase in BF content at both curing age of 28 and 90 days. Particularly, for the specimens with BF fractions of 1% and 2%, the improved integrity of the specimens due to the fiber reinforcement is more noticeable.

3.4 Flexural strength

Figure 7 depicts the impact of BF content and ATP as a cement substitute on the 28- and 90-day flexural strength of FC mixes containing 100% pumice aggregate (PA). As the curing age increased, strength augmentation was observed, as Fig. 7 illustrates. The addition of BF and the substitution of ATP for cement greatly increased the flexural strength; all ATP-incorporated mixes with BF showed greater flexural strength than the reference combination. More flexural strength was enhanced with increases in BF and ATP content; the maximum flexural strength was reached at 2% BF at each ATP content. The highest flexural strength was attained with 2% BF, where this fiber content offered optimal reinforcement. Furthermore, the pozzolanic reactivity of ATP helped form a denser and more robust matrix, enhancing resistance to flexural stresses. The reference mixture had the lowest flexural strength at both curing age of 28 and 90 days and the largest flexural strengths were found for the 30%ATP and 2%BF incorporated mixture which exhibited strength enhancement of 96.28 and 91.11% at 28 and 90 days, respectively, when compared to the reference mixture. According

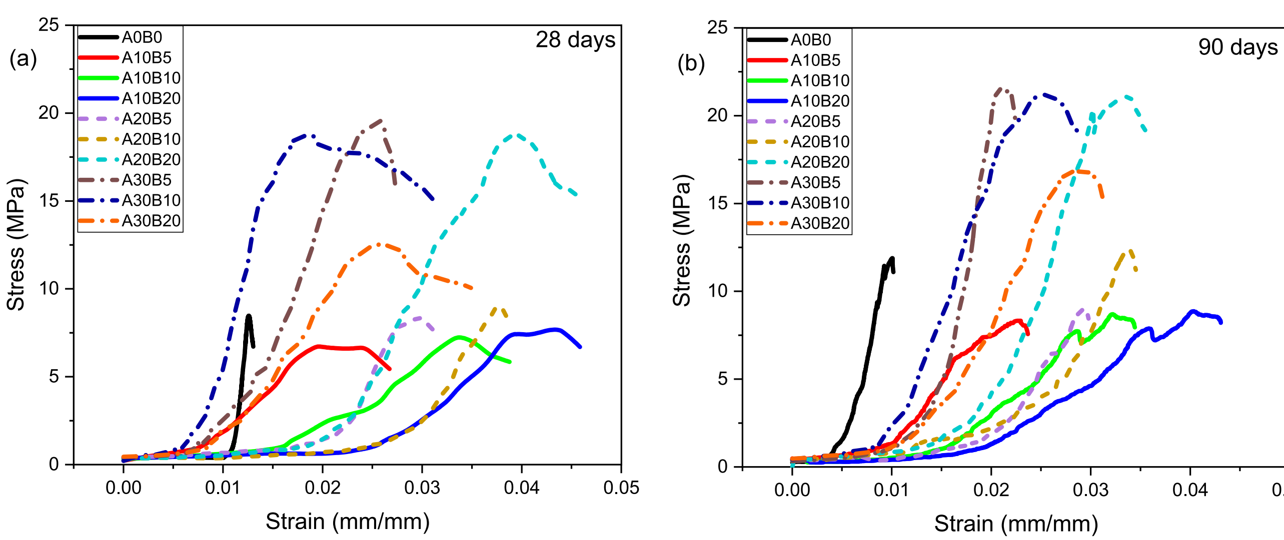

Fig. 6. 28- and 90-Day stress–strain behavior of FC mixtures

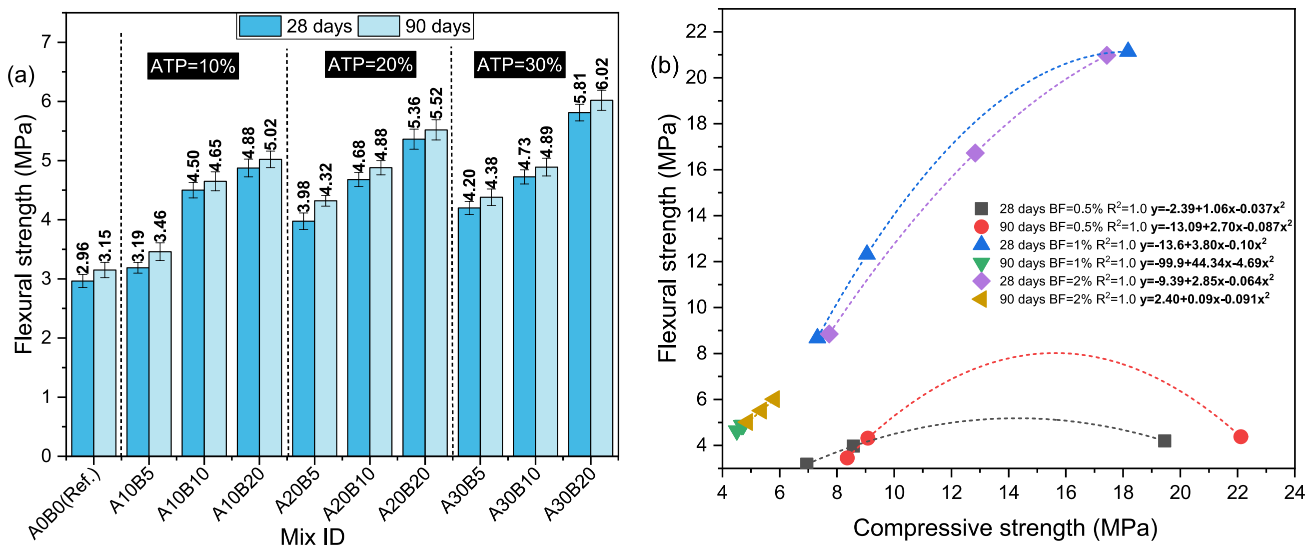

Fig. 7 **a** Results of flexural strength and **b** compressive vs. flexural strength

to Liu et al. [54], the compressive and flexural strengths of cement paste were improved by incorporating nano-ATP in the appropriate amount. This was partially explained by alterations to the mortar's pore structure, which reduced potentially hazardous pores and porosity. Alternatively, the pores can be filled in by the disorganized nano-attapulgite hydration activity of ATP, and its potential to boost cement paste's early stage bonding strength as well as its rod-like fibrous architecture, that could enhance fracture resistance, are the other reasons why it increases the flexural strength of the mortar [56]. The increase in flexural strength due to the BF can be attributed to the prevention of crack propagation by BF. Further emphasis was placed on the role that the fiber–matrix interfacial transition zone plays in the propagation of fractures [57]. Since BF had a high tensile strength, the enhancement in flexural strength can also be attributed to this property of BF. It was shown that the flexural strength of BF was positively correlated with its resistance to the mortar sample breaking [58]. Prior research has indicated that the flexural behavior of concrete and mortar can be markedly enhanced by the addition of fibers [59] ascribed to the excellent adherence of cementitious material to mixed BF, which helps to efficiently stop fracture propagation and improve flexural strength [33].

When 10% ATP-incorporated FC mixtures were considered, the mixture A10B20, which was incorporated with 2% BF, exhibited the maximum strength of 4.88 MPa and 5.02 MPa after 7 and 28 days of curing. This represents a 64.86% and 59.36% enhancement above the reference mixture. Similarly, when 20% ATP-included FC mixes were taken into account, the mixture A20B20—which was combined with 2% BF—showed the highest strength at 7 and 28 days of curing. Above the reference combination, this indicates an improvement of 81.08% and 75.23%. Combined use of ATP and BF improved the flexural strength notably due to the increase in the strong interface areas between the BF and binder matrix.

Figure 7b depicts the findings of measurements taken over 7 and 28 days for compressive strength and flexural strength. For each of the correlation factors, R^2 was determined to be 1.00 for all FC mixtures with 0.5,1 and 2% BF content at 28 and 90 days. There was a strong link between the FC mixes' compressive and flexural strengths.

3.5 Oven dry density

Figure 8 illustrates the impact of BF content and ATP as a cement substitute after 90 days on the oven dry density of FC mixtures containing 100% PA. The FC mixes displayed oven dry density values ranging from 1130 to 1642 kg/m^3, as illustrated in Fig. 8. According to the findings, the FC combinations with 20% ATP and 2% BF had the highest dry density (dry density enhancement of about 20%) in contrast to the reference combination that is devoid of BF and ATP, while the mixtures with 10% ATP and 0.5% BF had the lowest dry density with the dry density reduction of about 17% as compared to the reference blend. The dry density variation in this investigation was quite similar to the compressive strength change, since the w/b ratio and quantity of the foam agent were fixed. Put another way, the dry density increased as the compressive strength increased. Three mixtures A20B20, A30B5, and A30B10 which exhibited dry density values above 1600 kg/m^3 also indicated the largest compressive strength above 20 MPa at 90 days. The other two mixes containing 1 and 2% BF likewise showed a density drop of 3.5 and 7.4%, respectively, at 10% ATP content in

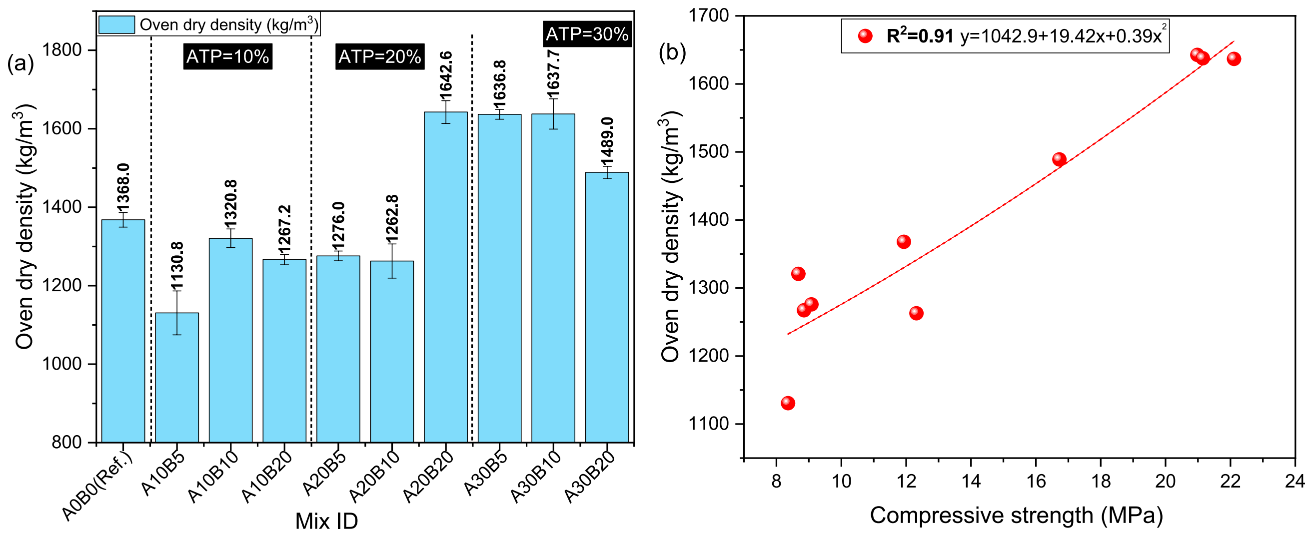

Fig. 8 **a** The results of dry density and **b**) the relation between compressive strength and dry density

comparison to the reference mixture. At 20% ATP content, the mixtures with 0.5 and 1% BF also revealed the density decline of 3.5 and 7.4%, respectively, but 2% BF incorporated mixture exhibited the largest dry density of 1642 kg/m^3 with a density enhancement of 20%. This improvement can be attributed the more compact, dense structure, and less porosity of the mixture.

At 30% ATP content, all mixtures exhibited larger dry density than the reference blend, the blends with 10% ATP, and 20%ATP-incorporated mixtures with 0.5 and 1%BF. Two mixes with 0.5 and 1% BF (A30B5 and A30B10) showed dry densities above 1600 kg/m^3 very slightly lower than the mixture with the largest density. These two mixtures depicted density enhancement of 19.59 and 19.66% as per the reference mixture. The combination containing 2% BF showed the dry density of 1489 kg/m^3 which also higher than the reference mixture with an enhancement of 8.8%. Combined use of 20%ATP in place of cement and 2%BF and 30%ATP with 0.5 and 1% BF was found to have the highest compressive strength that satisfies the criteria for structural bearing load strength, which ASTM C 330-17a [60] states must be greater than 17 MPa with densities above 1600 kg/m^3. It may be possible to employ the expressed FC mixtures in building applications. The FC blend containing 20% ATP and 2% BF achieved the highest dry density. This was due to ATP's pozzolanic reaction, which densified the matrix by filling voids with additional calcium silicate hydrate (C–S–H) gel, and the 2% BF content, which reinforced the structure by minimizing larger air gaps. In contrast, the blend with 10% ATP and 0.5% BF exhibited the lowest dry density, as the lower ATP content resulted in less densification, and the limited fiber reinforcement led to a more porous structure with increased air-filled spaces.

One of the main elements influencing compressive strength of foam concretes is density. Age, porosity, and dry density were found to affect the compressive strength of foamed concrete [61]. Figure 8b reveals that there was a 0.91 correlation coefficient between the dry density and compressive strength. The test findings reveal an excellent relationship between compressive strength and dry density.

3.6 The porosity and water absorption

Figure 9a illustrates the impact of BF content and ATP as a cement substitute after 90 days on the porosity and water absorption of FC mixtures containing 100% PA. Figure 9a illustrates the porosity range of the FC mixes, which was 9.7–16.6%. There was a range of 6.1–15.6% found in the FC mixes' water absorption. The mixture containing 30%ATP and 0.5%BF had the lowest porosity and water absorption with reductions of 40.0 and 56.73%, respectively, with respect to the reference mixture. This decline makes sense by the mixture's more compact and dense structure, which also had the highest compressive strength. However, the blend with 10%ATP and 1%BF had the largest porosity with an increase of 4.4%, and the mixture with 10%ATP and 0.5%BF had the largest water absorption with an increase of 10.6%. All 10%ATP-incorporated mixtures exhibited larger porosity and water absorption that the reference mixture. Conversely, all 20 and 30%ATP –incorporated mixtures revealed lower porosity and water-absorption results with respect to the reference mixture. Addition of BF affected the porosity and water absorption positively or negatively depending on the ATP and BF content. At 10%ATP content, inclusion of 2%BF resulted in lowest porosity and inclusion of 1%BF led to the lowest water absorption. At 20%ATP content, increase

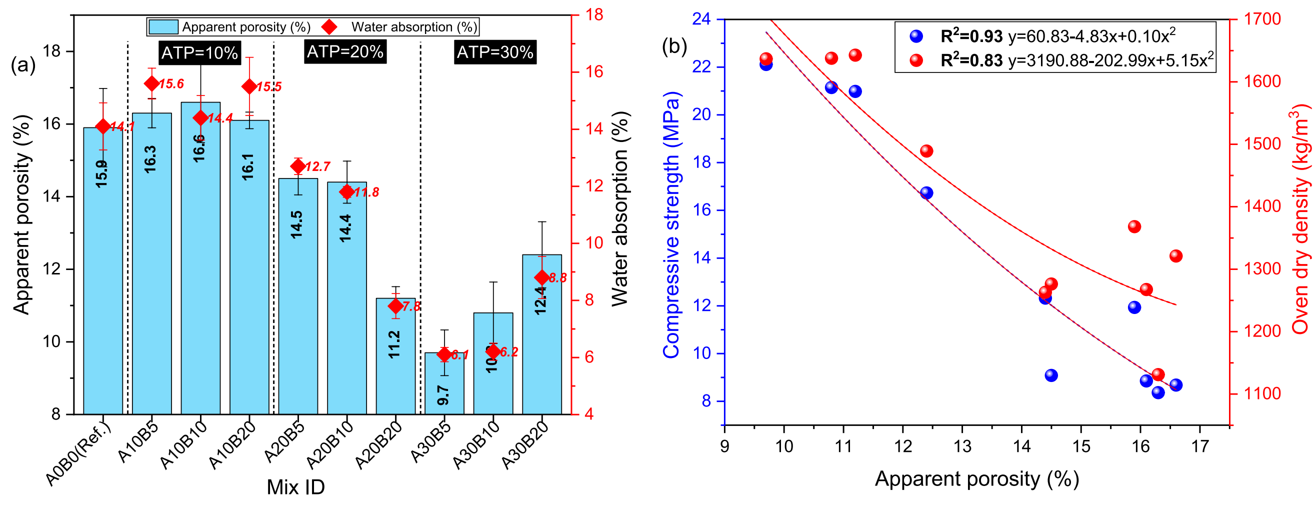

Fig. 9 Apparent porosity and water absorption (**a**), and correlation between porosity, strength, and dry density (**b**)

in BF content reduced the both values notably and the lowest results were achieved at 2%BF incorporated mixtures. On the other hand, at 30% ATP content, increase in BF content enhanced the both values and the largest results were achieved at 2%BF incorporated mixtures. Fiber insertion has two distinct effects on porosity. First, a larger pore size results from the infiltration of fiber into the aggregate dispersion. The enlargement is usually influenced by the elasticity of the fiber modulus. Nonetheless, by filling the empty space with fiber, the porosity might be reduced [62]. As expressed, using 10% ATP in place of cement enhanced the porosity and absorption slightly but replacing cement with 20 and 30%ATP decreased the water absorption and porosity. The hydration reaction of the cement mortar may be accelerated by the nano-attapulgite, producing more calcium C–S–H gels, according to a study by Lindgreen et al. [63]. This would result in a decrease in the size and quantity of pores in the mortar while also increasing its density. Through the promotion of cement secondary hydration, the pozzolanic activity of calcined nano-ATP can significantly increase the compressive strength of concrete while reducing its porosity and water absorption. The mixture containing 30% ATP and 0.5% BF had the lowest porosity and water absorption, attributed to ATP's high pozzolanic reactivity at this level, which densified the matrix by filling voids with C–S–H gel. In contrast, mixtures with 10% ATP showed higher porosity and water absorption, because the lower ATP content resulted in less matrix densification. Furthermore, the blend with 10% ATP and 1% BF likely exhibited increased porosity due to fiber clustering, while the 10% ATP and 0.5% BF mix had the highest water absorption due to limited matrix compaction.

One of the main elements influencing compressive strength of foam concretes is density. Age, porosity, and dry density were found to affect the compressive strength of foamed concrete [61]. Figure 9b reveals that there were 0.93 and 0.83 correlation coefficients between the porosity, compressive strength, and dry density, respectively. The test findings reveal that the porosity, compressive strength, and dry density are clearly correlated. The porosity increased as the compressive strength and dry density decreased.

3.7 Thermal conductivity

One of the most important aspects of building design and construction is making sure there is enough thermal insulation. Foam concrete's cellular structure gives it excellent thermal insulation qualities. The degree to which thermally conductive foam concrete is affected by pore size, density, aggregate type, fiber content, and mineral admixtures [2].

Figure 10a illustrates the impact of ATP as a cement substitute and the amount of BF on the thermal conductivity of FC mixtures containing 100% PA after 90 days. The results displayed in Fig. 10a demonstrate that the FC mixes' thermal conductivity ranged from 0.606 to 0.741 (W/mK). Because the porosity and dry density of the specimens have a significant impact on thermal conductivity, lower dry density corresponds to higher porosity and lower thermal conductivity. The blend with 10%ATP and 0.5%BF which had the lowest dry density exhibited the least thermal conductivity 4.2% lower than the reference blend. With the lowest porosity, the blend containing 30% ATP and 0.5% BF showed the maximum thermal conductivity, 17.06% more than the reference mixture. The differences in thermal conductivity between the FC blends containing 10% and 30% ATP and 0.5% BF were due to variations in density and porosity. The blend with 10% ATP and 0.5% BF had a lower density and higher porosity, which created additional air pockets that served as

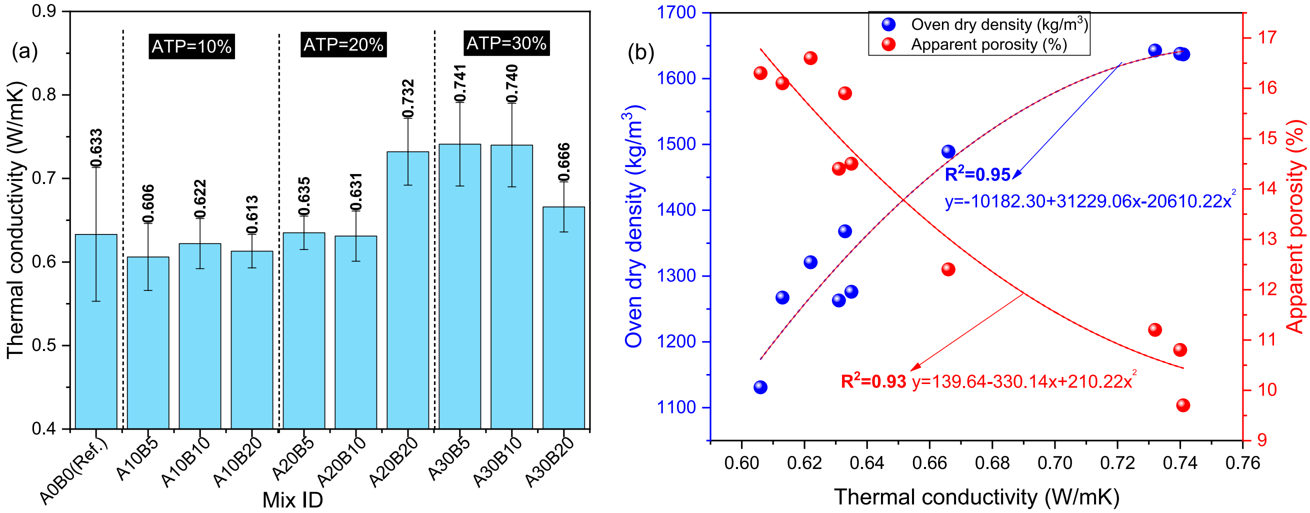

Fig. 10 **a** The results of thermal conductivity and **b** thermal conductivity vs. dry density and porosity

insulators, leading to a 4.2% reduction in thermal conductivity compared to the reference mixture. Conversely, the blend with 30% ATP and 0.5% BF featured a denser, less porous matrix as a result of ATP's pozzolanic reaction, which filled voids and enhanced heat transfer through the solid material, causing a 17.06% increase in thermal conductivity. All mixtures containing 10%ATP as a cement replacement revealed lower thermal conductivity values varying from 0.606 to 622 (W/mK) compared to the reference mixtures. Having higher porosity, lower dry density, and compressive strength of these mixtures supported these results. The mixtures containing 0.5 and 1% BF similarly showed very slightly greater and lower thermal conductivity values than the control mixture at 20% ATP concentration, respectively, but the thermal conductivity of the mixture with 2%BF increased by 15.6% parallel to the incline in the dry density and compressive strength.

At 30%ATP content, thermal conductivity values of the blends with 0.5 and 1%BF were the highest with the enhancement of about 17% parallel to the increase in the dry density and compressive strength with respect to the control blend and the thermal conductivity of the blend with 2%BF decreased slightly as compared to the other two blends with 30%ATP. The blend with 10% ATP and 0.5% BF exhibited the lowest thermal conductivity, attributed to its higher porosity and lower density, which formed insulating air pockets that limited heat transfer. In contrast, the blend with 30% ATP and 0.5% BF displayed the highest thermal conductivity due to its denser, less porous structure, enabling easier heat flow through solid material pathways.

Figure 10b reveals that there were 0.95 and 0.93 correlation coefficients between the thermal conductivity, dry density, and porosity, respectively. The results of the tests indicate that the thermal conductivity, dry density, and porosity are clearly correlated. The thermal conductivity increased as the dry density increased and porosity decreased.

3.8 Sorptivity

Sorptivity is the capacity of a porous material to extract water from a free water source and transfer it through capillarity. All three methods are highly dependent on the pore volume and the pore network's connection [64]. The water sorptivity/absorption rate is a suitable measure of the fluid transport properties of building materials and, hence, a trustworthy indicator of material durability [65]. A decline in this rate consistently indicates increased durability. Sorptivity seems to be a more helpful criterion than permeability for categorizing the performance of concrete [66].

The effects of BF content and ATP as a cement substitute on the sorptivity of FC mixes containing 100% PA after 90 days are shown in Fig. 11a. As illustrated in Fig. 10a, the sorptivity of FC mixtures ranges from 3.22 to 6.88 kg/m^2. The statistics on porosity, oven dry density, and compressive strength that were previously discussed in the sections above were perfectly consistent with the sorptivity results. The blend with the greatest compressive strength, 30%ATP and 0.5%BF, also had the lowest sorptivity, 50.53% less than the reference blend. With the largest porosity, the mixture containing 10% ATP and 1% BF showed the maximum sorptivity, 5.7% higher than the reference mixture. At 10%ATP content, the sorptivity increased by 3.2 and 5.7% at 0.5 and 1%BF content, respectively, and decreased by 0.3% at 2%BF content compared to the reference mixture. When 20%ATP was added instead of cement, all mixtures had lower sorptivity and 2%BF incorporated mixture achieved the sorptivity of 3.89 kg/m^2 showing the 40.2% reduction with respect to

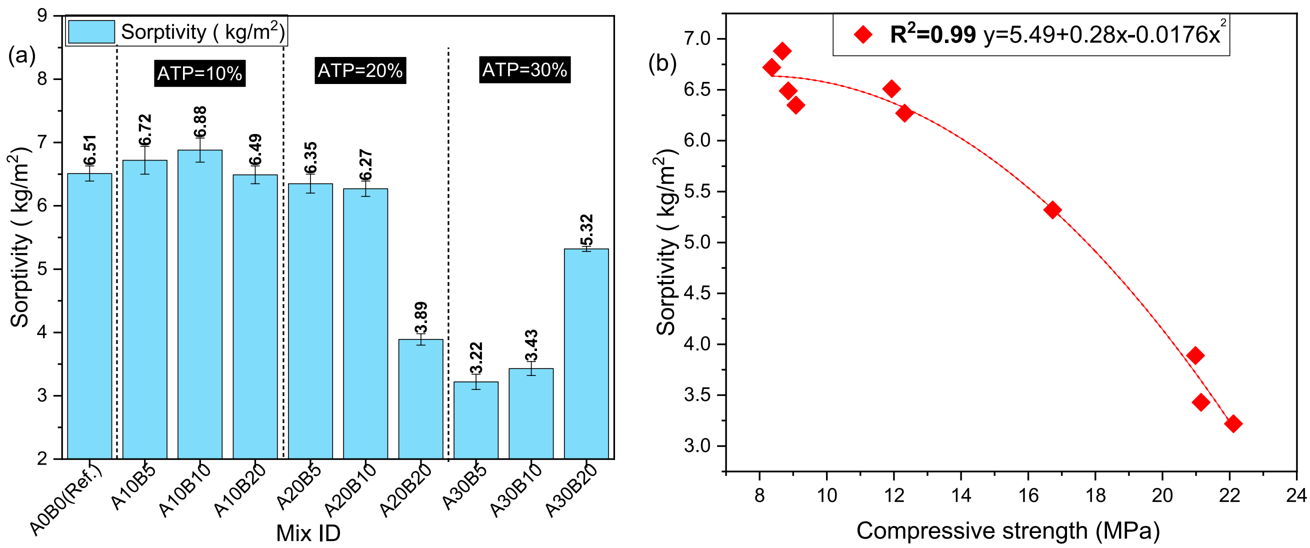

Fig. 11 **a** Sorptivity outcomes and **b** strength vs. sorptivity of FC mixtures

the reference mixture. All mixes exhibited also reduced sorptivity when 30% ATP was added in place of cement; the mixture incorporating 0.5% BF which had also the largest compressive strength attained the lowest sorptivity of 3.22 kg/m^2 due to the formation of more compact and dense structure resulting from the combined use of 30%ATP and 0.5%BF [62], indicating a 50.53% drop in comparison to the reference mixture. Through the production of additional calcium silicate hydrate (C–S–H), the nano-attapulgite can accelerate the hydration reaction of cement mortar, reducing the amount and size of pores while increasing the density of the mortar. The pozzolanic activity of calcined nano-attapulgite can promote the secondary hydration of cement, increasing the unit weight and compressive strength of regular concrete [63].

Figure 11b illustrates the relation between the compressive strength and the sorptivity values and a very strong correlation coefficient R^2 of 0.99 was found between them indicating a clear correlation between sorptivity and compressive strength as demonstrated by the test results.

3.9 Microstructure analyses for 28-day water-cured specimens

Figure 12 reveals the microstructure of the reference blend A0B0 at various magnifications. SEM images show that the cement matrix is dense. In addition, pumice aggregates embedded in the matrix are visible. It was determined that the cellular structure was formed thanks to the foam used in the mixtures. Because the presence of independent spherical

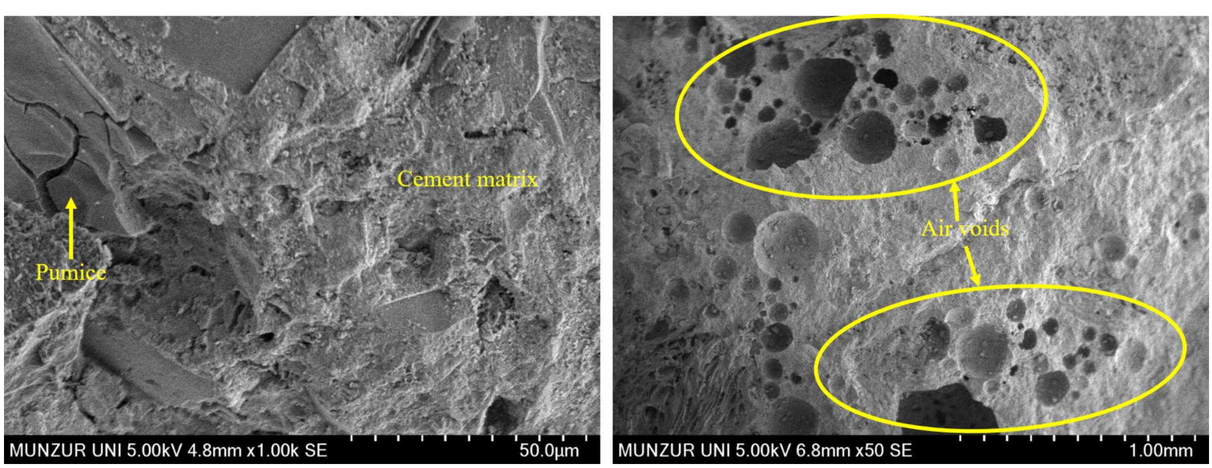

Fig. 12 Microstructure of A0B0 mixture

air bubbles was observed. The diameter of these voids decreases up to 20 µm. The thermal conductivity coefficient of the A0BO mixture was 0.633 W/m K, and the 28-day compressive strength was measured as 8.48 MPa.

Figure 13 shows the microstructure of the A10B10 mixture. SEM image with 250 × magnification shows the surface of pumice aggregate. It is observed in these images that the pumice aggregate has a porous structure. In addition, the presence of BF was frequently observed in SEM analyses. The presence of hydration products formed due to the reaction of cement with water was detected on the BF surface. It was observed that these products adhered to the fiber surface during fiber debonding. This proves that the adherence between BF and matrix is relatively good. Comparing the A10B10 mixture to the reference blend, the 28-day flexural strength rose 1.85 times.

Figure 14 depicts the SEM of the A30B20 blend at different magnifications. SEM images at 250 × magnification show that BFs are locally densified. This appearance is due to the agglomeration tendency of BF. In addition, the hollow surface of the pumice aggregate was also observed in SEM images. These voids are usually independent of each other. This situation affects the thermal performance of foam concretes. For instance, the A30B20 blend's thermal conductivity coefficient rose by around 1.1 times when compared to the reference combination. This is because the attapulgite used in the blends enhances the cake volume and decreases the pumice content. As a result, the thermal conductivity coefficient increases relatively.

3.10 The resistance of FC mixtures to high temperature

3.10.1 Compressive strength

Figure 15a illustrates the impact of ATP as a cement substitute and basalt BF concentration on the average compressive strength of FC mixtures containing 100%

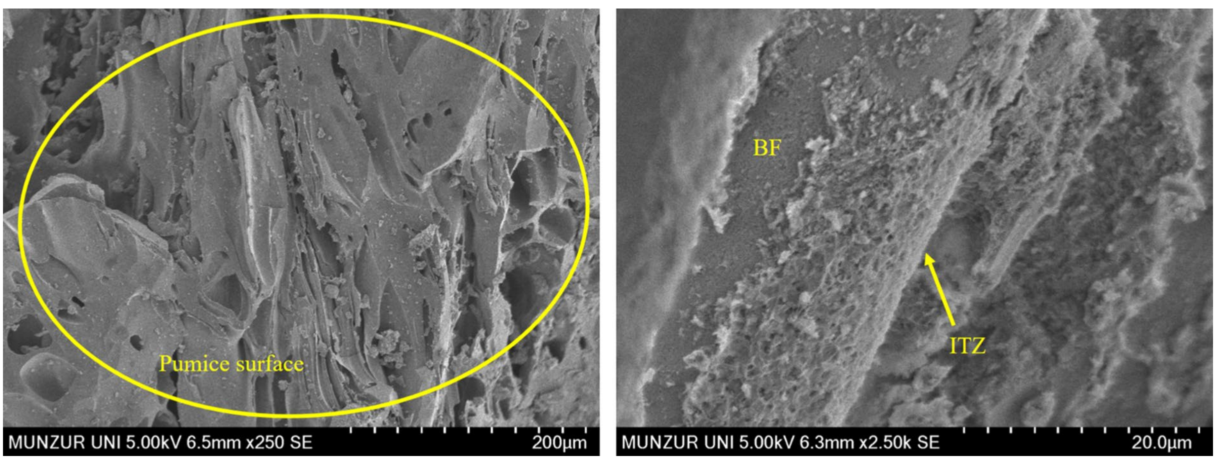

Fig. 13 Microstructure of A10B10 mixture

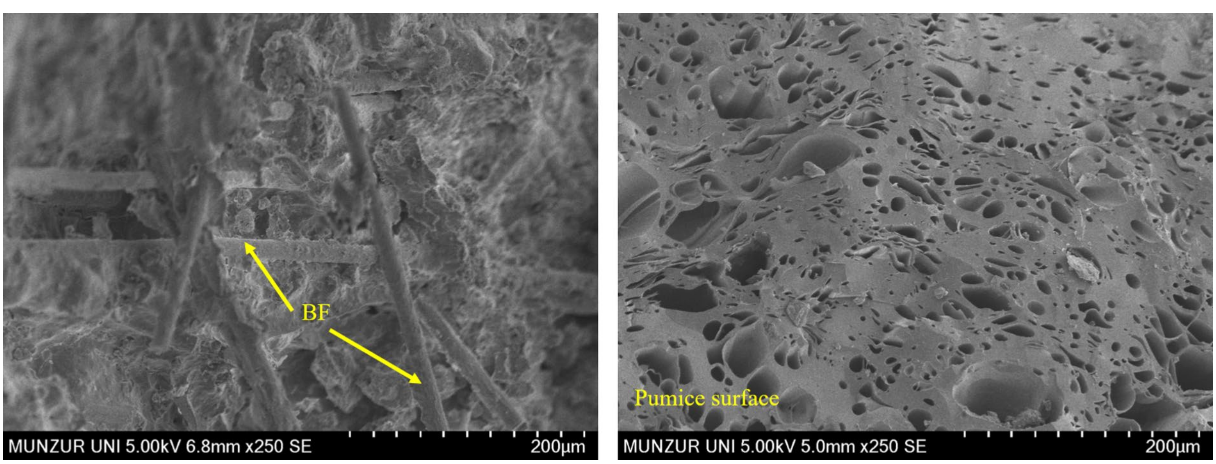

Fig. 14 Microstructure of A30B20 mixture

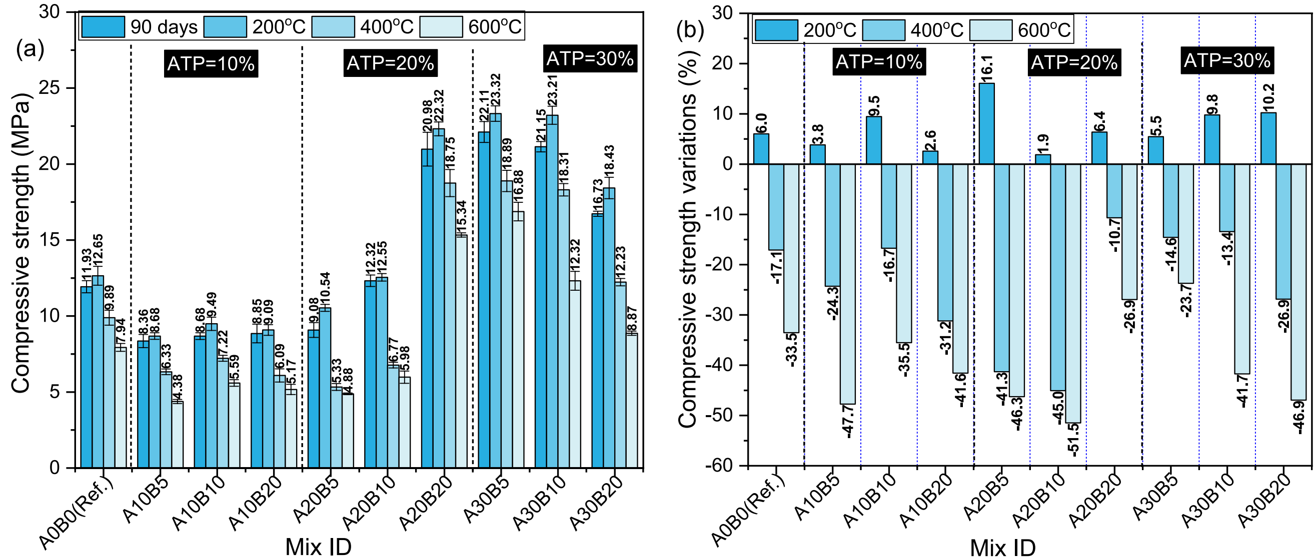

Fig. 15 **a** The compressive strength outcomes and **b** change in strength variations on exposure to high temperature

PA following exposure to high temperatures. Figure 15b shows the strength fluctuations when comparing the compressive strength values obtained on exposure to high temperatures with those cured after 90 days. When the compressive strength on the exposure to 200 °C was compared to the strength at 90 days, the reference mixtures and the blended mixtures of ATP and BF both shown an increase in strength. Results demonstrate that applying 200 °C to FC specimens increased their compressive strength. This improvement was mostly ascribed, in the literature, to the hydration of anhydrous cement and the accelerated pozzolanic process [67]. The strength of all mixtures, however, decreased when they were subjected to the high temperature of 400 and 600 °C. Regular exposure to extremely high temperatures weakens concrete for a number of causes, all of which have been extensively studied in the literature. It is thought that several physicochemical alterations inside the concrete matrix are what lead to degradation in the case of a fire. The main causes of strength loss are aggregate disintegration, dehydration with concurrent matrix cracking, and the breakdown of calcium hydroxide (CH) and calcium silicate hydrate gel (CSH) [3]. The thermal performance of FC mixtures was reduced by substituting 10%ATP for cement when compared to the reference combination at 400 and 600 °C. The blend containing 10%ATP and 1%BF demonstrated the highest thermal performance across all high temperature exposures, demonstrating a 9.5% rise in strength at 200 °C and strength loss of 16.7 and 35.5% at 400 °C and 600 °C. 10%ATP-incorporated mixture with 0.5%BF which had also the lowest compressive strength exhibited the worst thermal performance at 600 °C with a strength loss of 47.7%.

When 20% ATP was substituted for cement, the thermal performance of FC mixtures with 0.5 and 1%BF was much lower than that of the reference combination at 400 and 600 °C. However, the mixture containing 2% BF demonstrated the best thermal performance across all high temperature exposures, with a 6.4% strength increase at 200 °C and a 10.7% and 26.9% strength loss at 400 °C and 600 °C, respectively. FC mixes with 0.5%BF provided the highest thermal performance with the least amount of strength loss at 600 °C when 30% ATP was used in place of cement. However, the mixture containing 2% BF demonstrated the worst thermal performance, with a 46.9% strength loss at 600 °C.

When ATP was used in place of cement, the strength loss upon exposure to high temperatures was frequently reduced, especially at 10% ATP content, as Fig. 15 illustrates. This is due to the fact that high temperatures, between 400 and 600 °C, alter the mineral composition of ATP and lead to the calcination and dissolution of SiO_2, which alters the hydration activity of materials that contain cement [68].

3.10.2 Stress–strain behavior after high temperature

Figure 16 depicts the impact of basalt fibers (BF) content and attapulgite powder (ATP) as a cement substitute on the axial stress–strain behavior of FC mixes at 200, 400 and 600 °C. As expected, Stress decrease was noticed with an increase in high temperature, as shown in Fig. 16 but strain was enhanced with the increase in high temperature. Peak stress values were the same as the compressive strength

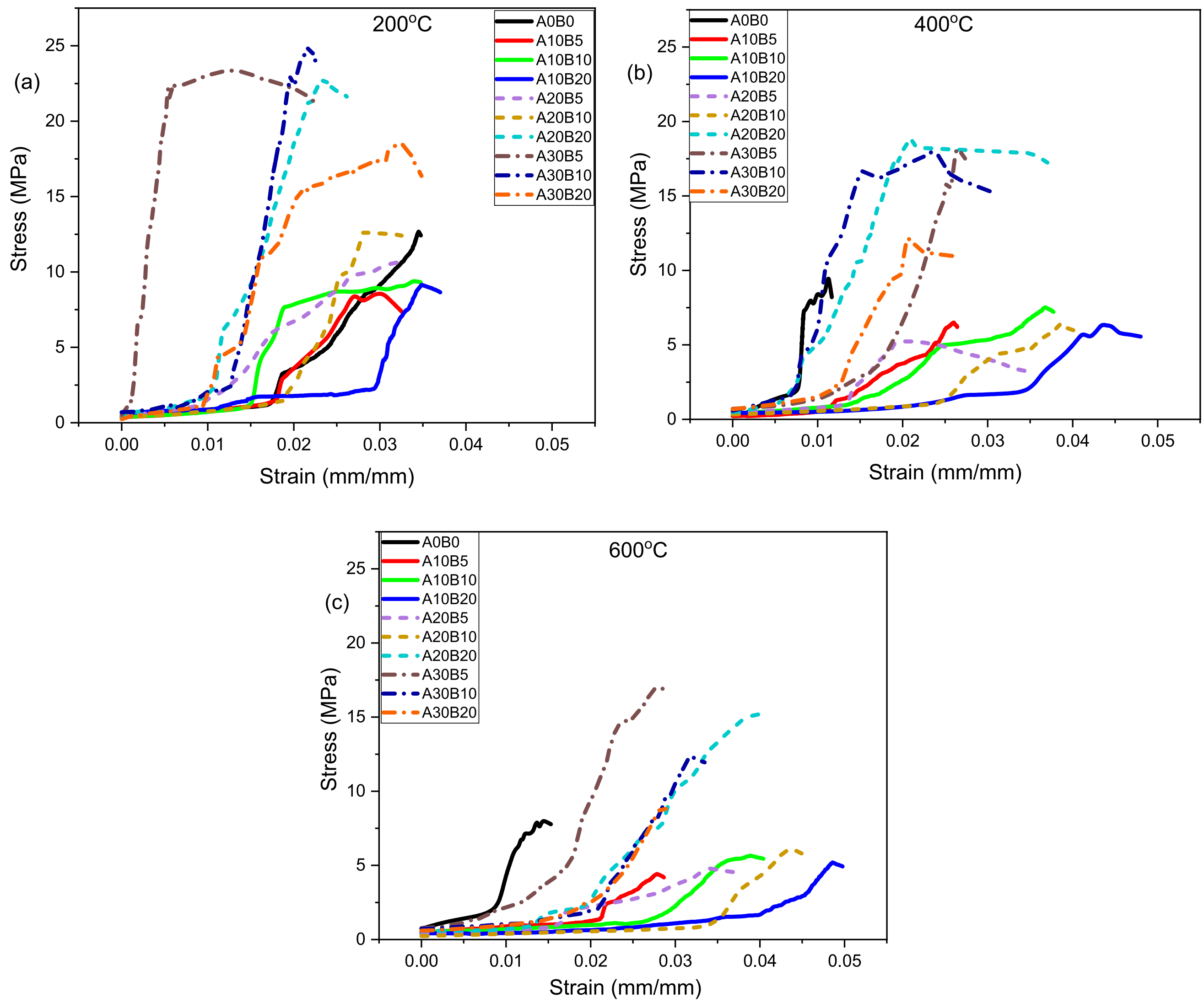

Fig. 16 Stress–strain behavior of FC mixtures after **a** 200, **b** 400, and **c** 600 °C

values illustrated in Fig. 15. At 200 °C, the blend containing 30%ATP and 0.5%BF (A30B5) exhibited a sharp increase in stress values with a very small strains. After reaching peak stress, a large strains happened with a slight increase in stress then failed at strain value of above 0.02. On the other hand, other mixtures generally exhibited large strains with a low stress increment during the initial loading period and then stress increase up to the peak stress. More strains can be recorded for the mixtures comprising 10%ATP with relatively low stress values. With an increase in BF content, more strains were also observed following peak strains. At 400 °C, all mixtures had lower peak stress than the mixtures exposed to 200 °C, but as expected, more peak and ultimate strains were gained for the mixtures containing BF due the high-temperature resistance of BF showing bridging behavior and prevented high-temperature-induced cracks [69]. The reference mixture exhibited the lowest ultimate strain, whereas the blend with 10%ATP and 2%BF indicated the largest ultimate strain on exposure to 400 °C. The mixture with 0.5%BF and 30%ATP which had one of the largest peak stress indicated an approximately linear stress–strain behavior until the peak stress then failed without strain after peak stress. On the other hand, the mixture with 2%BF and 20%ATP which had the largest peak stress exhibited more rigid stress–strain behavior until the peak stress then the strain increased with a slight decrease in stress and reached the strain of nearly 0.04 before failure. At 600 °C, all mixtures exhibited more peak stress loss than the mixtures exposed to 200 and 400 °C but as expected, because BF exhibits bridging behavior at high temperatures and inhibits cracks caused by high temperatures, mixtures containing BF achieved greater peak and ultimate stresses. Strains increased more with the slight increase in stress. When exposed to 600 °C, the blend comprising 10% ATP and 2% BF showed the biggest ultimate strain, whereas the reference mixture showed the lowest ultimate strain. The combination containing 0.5%BF and 30%ATP had the highest peak stress values, suggesting a somewhat linear stress–strain behavior up until the peak stress, after which the mixture broke without strain.

3.10.3 Weight loss on the exposure of high temperature

Figure 17a shows the impact of ATP as a replacement for cement and BF amount on the mean loss of weight of FC blends, comprising 100% PA, upon exposure to high temperatures. The reduction in weight is a result of decomposition, spalling, and moisture loss through hydration products. The weight loss increases as temperature rises and accelerates beyond 200 °C, as evident in Fig. 17a. The weight loss of FC mixes was mainly dependent on the amount of BF and ATP. The weight loss of FC mixtures after high temperatures is influenced by density. Greater mass loss in foamed concrete is also a function of increased porosity and moisture content [70]. This is the reason that the mixtures that showed the biggest porosity and lowest dry density also showed the largest weight loss. It seems that replacing cement with ATP tends to decrease the weight loss of the mixtures and 30%ATP-incorporated mixtures exhibited the lowest weight loss. The ATP concentration was the primary determinant of the effect of BF on the weight loss of the combinations following high temperature. When cement was replaced with 10%ATP, all mixtures revealed larger weight loss than the reference mixture and the mixture with 0.5%BF which had the lowest compressive strength demonstrated the maximum weight loss on temperature exposure of 200, 400 and 600 °C. Increasing content of BF tended to decrease the weight loss for the mixtures with 10%ATP. The mixes with 0.5 and 1%BF showed greater weight loss than the reference mixture when cement was substituted with 20%ATP, and the blend with 2%BF, which had the compressive strength above 20 MPa at 90 days, had lower weight loss at 200, 400, and 600 °C than the reference mixture. For the mixes with 30%ATP, all mixtures showed lower weight loss than the reference blend and the blends with 10%ATP. Adding more BF tended to increase the weight loss and maximum weight loss was determined for the 2%BF incorporated blend. Figure 17b indicates the compressive strength and weight loss relation on exposure to high temperature. Extremely high correlation values R^2 of 0.98, 0.94, and 0.97 were ascertained between the compressive strength and weight loss of the samples at 200, 400, and 600 °C, respectively, showing a parabolic relationship with the increase in strength corresponding to the weight loss decrease.

3.10.4 Microstructure after 600 °C

The A0B0 mixture's microstructure alterations after being subjected to 600 °C are depicted in Fig. 18. It became apparent that the effect of the high temperature led to the formation of micro-cracks in the matrix. Nonetheless, it was noted that the matrix remained dense. Even its adherence to pumice was observed to be good. In SEM images, it was observed that spherical air bubbles were formed, and these bubbles were independent of each other. In this way, the heat propagation caused by high temperatures is reduced. This reduced the damage to the microstructure. High-temperature exposure led to the formation of

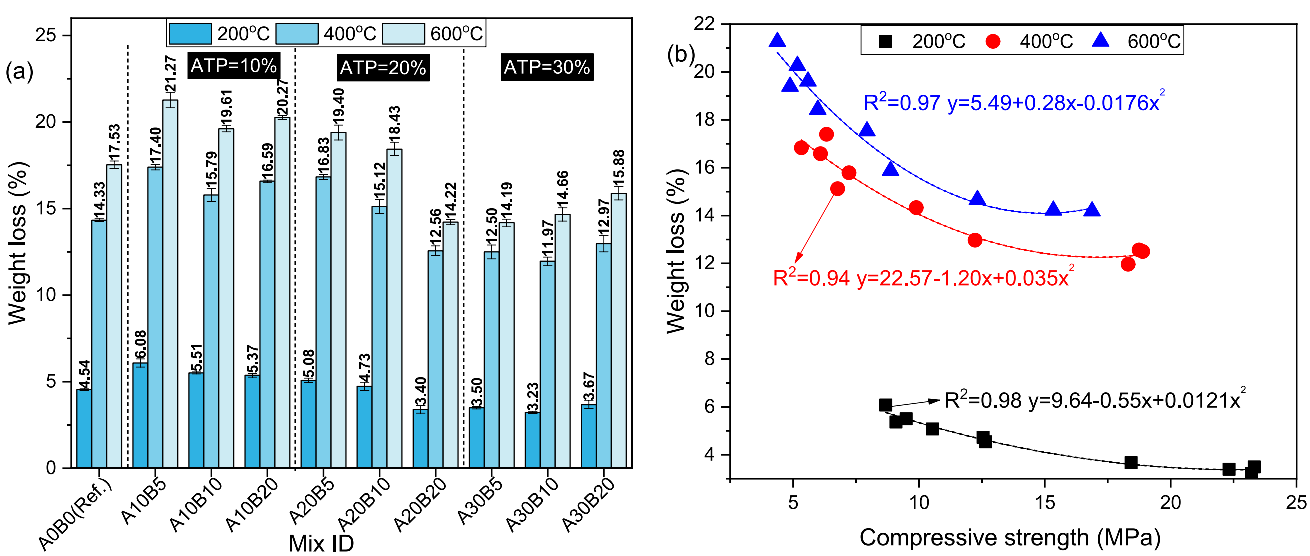

Fig. 17 **a** Weight loss and **b** compressive strength vs. weight loss of FC samples after high temperature

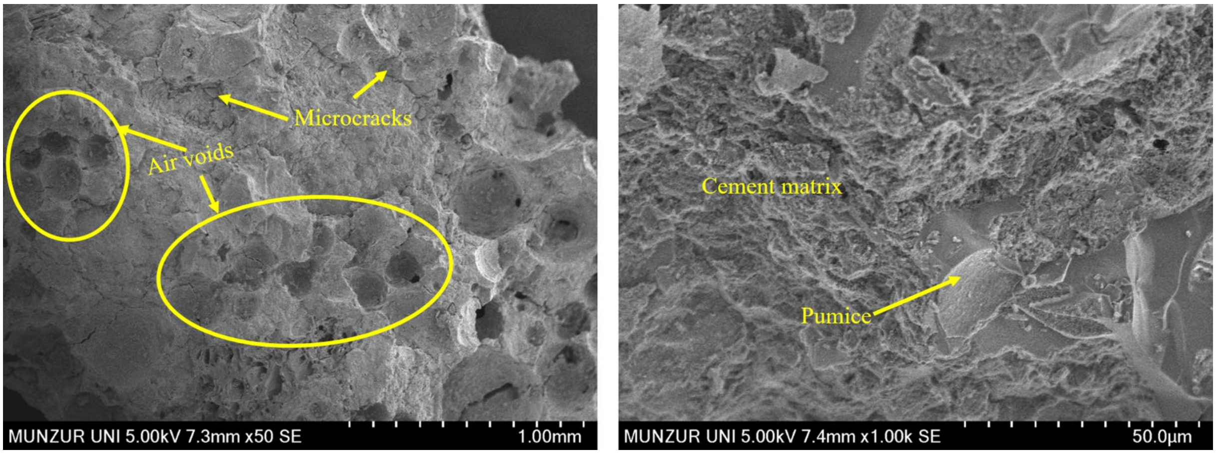

Fig. 18 Microstructure of A0B0 mixture

micro-cracks in the cement matrix; however, the matrix remained relatively dense, and the bond between the cement and pumice particles was well preserved. Spherical air voids were also observed, potentially enhancing the material's thermal insulation properties. Micro-cracks are a common response of cementitious materials to heat, as thermal expansion induces internal stresses that can lead to cracking. The extent of cracking depends on factors, such as material composition, heating rate, and maximum temperature. The maintenance of matrix density indicates that the structural integrity was not significantly compromised, contributing to the material's mechanical strength and durability. Strong adherence between the cement matrix and pumice is crucial for stress transfer and preventing particle detachment. The spherical air voids further improve thermal insulation by reducing thermal conductivity and minimizing stress concentrations, which lowers the risk of additional cracking. The A0B0 mixture exhibits reasonable thermal stability and resistance to high temperatures. Although micro-crack formation is not ideal, it did not significantly degrade the material's properties. The effective bond between the matrix and pumice, along with the presence of air voids, positively influences the material's overall performance.

The microstructure of the A10B10 blend exposed to high temperature is given in Fig. 19. As in other blends, it was observed that BF agglomerated in some regions. In addition, pumice aggregate with a hollow structure was observed in 50 × magnification SEM images. Micro-cracks were not observed in the matrix. The reason for this is that BF prevents crack propagation. The A10B10 blend reached a compressive strength of roughly 5.5 MPa at 600 °C after that.

The SEM image of the A30B20 mixture is shown in Fig. 20. Fiber agglomeration was observed in this blend using 2% BF. The distance between two BFs was measured as 35 µm in the SEM image. Spherical air bubbles formed in other blends were also observed in this blend. BF and these air bubbles reduced the damage caused by high

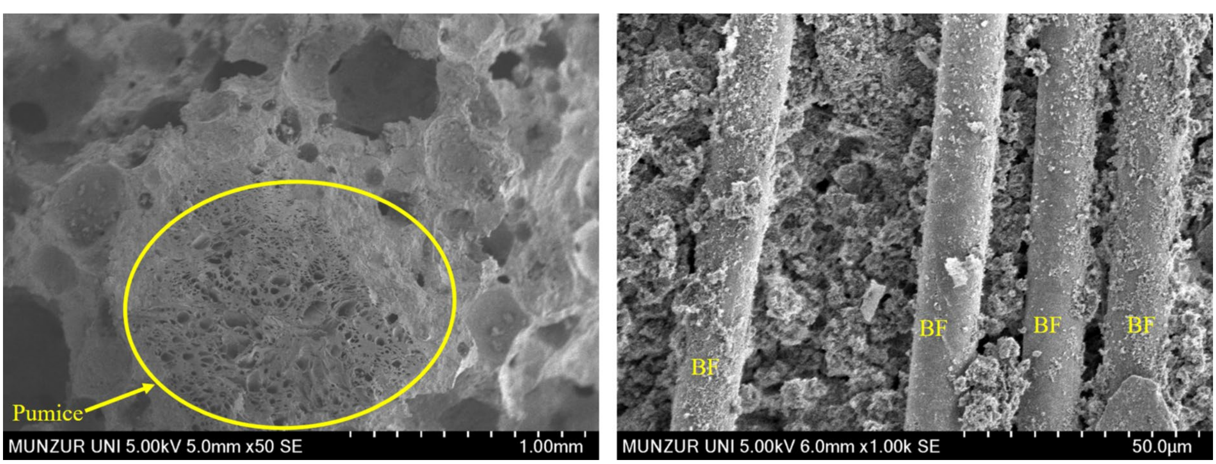

Fig. 19 Microstructure of A10B10 mixture

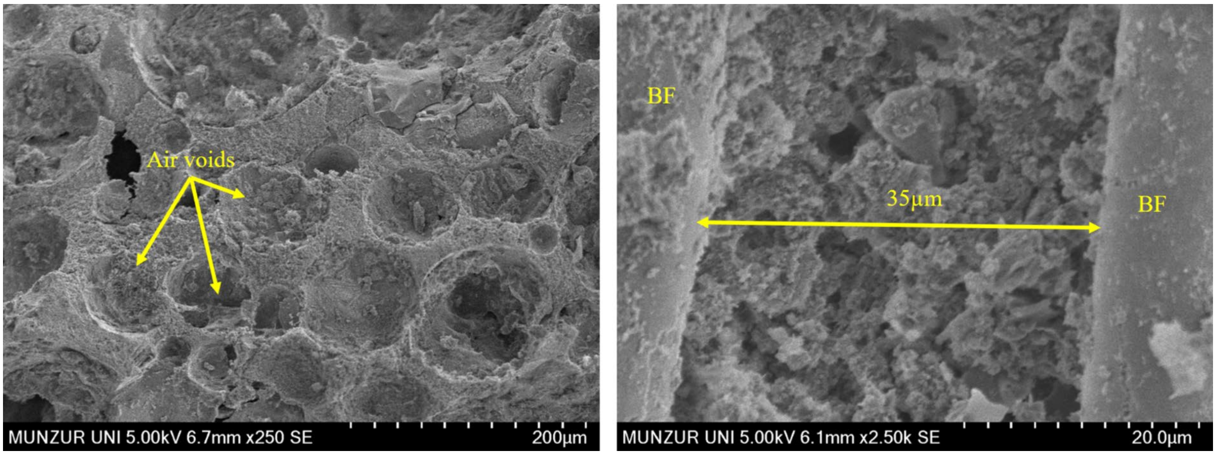

Fig. 20 Microstructure of A30B20 mixture

temperatures. As a matter of fact, map cracks that may occur due to high temperature were not observed in the matrix.

3.11 Resistance to sulfate attack

3.11.1 Compressive strength

A prevalent issue with concrete's durability is sulfate attack, which can lead to various problems such spalling, increased permeability, cracking, and loss of strength. Once sulfate ions and hydration products penetrate interior pores, a chemical reaction takes place that produces ettringite and gypsum as the final products [71]. Following 90 of exposure to 5% $MgSO_4$, the compressive strength and weight loss of FC mixtures were evaluated to determine the effect of the attack.

The effects of ATP as a cement substitute and BF concentration on the average compressive strength of FC blends comprising 100% PA after being subjected to the sulfate assault over a 90-day period are depicted in Fig. 21a. Figure 21b illustrates the differences in compressive strength between the 90-day FC combination results and the results following sulfate attack. All FC mixtures exhibited strength loss ranging from 6.2 to 40.1% on the exposure to sulfate attack. The blend comprising 10% ATP and 1% BF indicated the least strength loss, whereas the blend containing 20% ATP and 1% BF produced the greatest strength loss. The blend containing 10% ATP and 1% BF exhibited the least strength loss due to an optimal combination of matrix densification and crack resistance, which effectively limited sulfate ingress and expansion. In contrast, the blend with 20% ATP and 1% BF experienced the greatest strength loss, likely

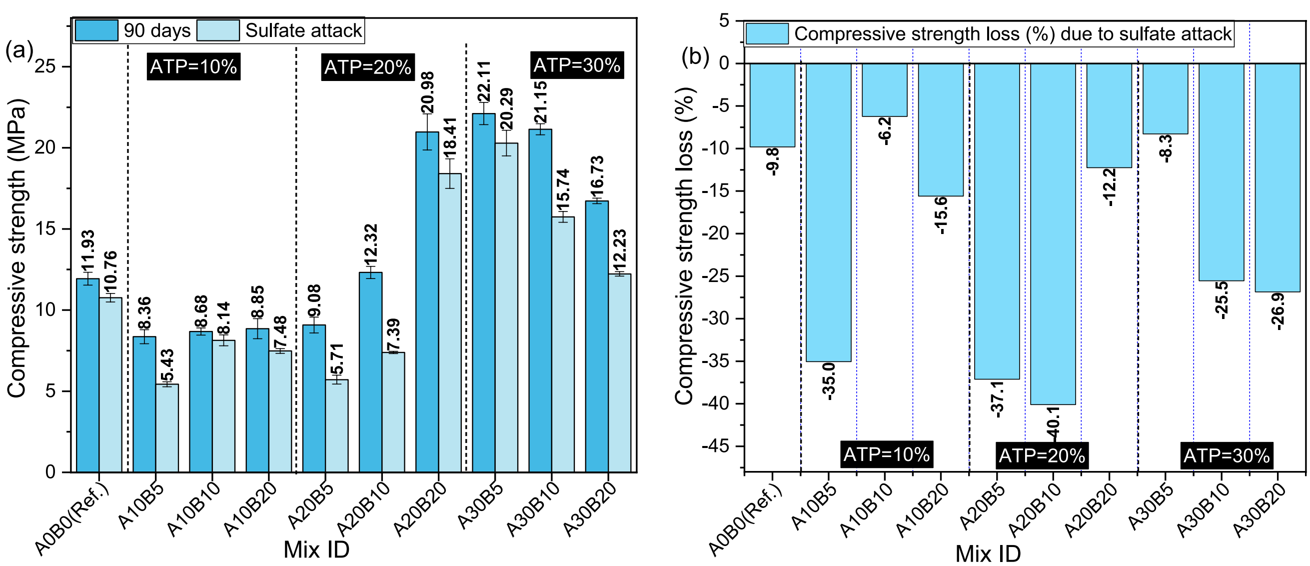

Fig. 21 **a** The compressive strength findings and **b** change in strength on the exposure of sulfate attack

because the higher ATP content led to a less cohesive matrix, rendering it more susceptible to sulfate-induced damage, even with the reinforcement provided by BF. Strength loss mainly depended on the BF content. When cement was replaced with 10%ATP, the mixture with 0.5%BF revealed the worst sulfate resistance showing strength loss of 35%. On the other hand, the greatest sulfate resistance was found in the mixture containing 1%BF, which showed a 6.2% strength decrease. When 20%ATP was used in place of cement, the combination containing 1%BF showed the weakest sulfate resistance, with a 40.1% reduction in strength. However, the mixture with 2%BF, which had a 12.2% strength loss, had the highest sulfate resistance. The mixture containing 2%BF exhibited the worst sulfate resistance when 30%ATP was substituted for cement, with a 26.9% drop in strength. However, sulfate resistance was best in the mixture containing 0.5%BF, with an 8.3% strength loss. The principal reason for this low strength loss is because the pozzolanic and filling properties of 30%ATP and 0.5%BF restrict the permeability of concrete, impeding the ingress of harmful ions and postponing the degradation of concrete subjected to harsh conditions like acid and sulfate attacks [72].

3.11.2 Stress–strain behavior

Figure 22 depicts the impact of BF content and ATP as a cement substitute on the axial stress–strain behavior of FC mixes after sulfate attack for 90 days. Stress loss was noticed for all mixtures when compared the strength values at 90 days. The reference mixture exhibited a linear stress–strain behavior until the peak stress then failed without strain. The reference mixture also exhibited the lowest ultimate strain, whereas the blend with 10%ATP and 2%BF indicated the largest ultimate strain on exposure to sulfate attack. The blend with 0.5%BF and 30%ATP which had the largest peak stress indicated an approximately linear stress–strain behavior until the peak stress. The mixture with 0.5%BF and 30%ATP also had the second lowest ultimate strain after the reference mixture. However, the blend with 2%BF and 10%ATP revealed the largest ultimate strain with a modest rise in strain after peak stress before failure. The worst stress–strain behavior was observed for the blend comprising10%ATP and 0.5%BF showing an increase in stress and strain up to the peak stress and then declined in stress with increasing strain. The mixture with 2%BF and 20%ATP exhibited the second largest peak stress with an approximate stress–strain behavior with a strain value of about 0.035.

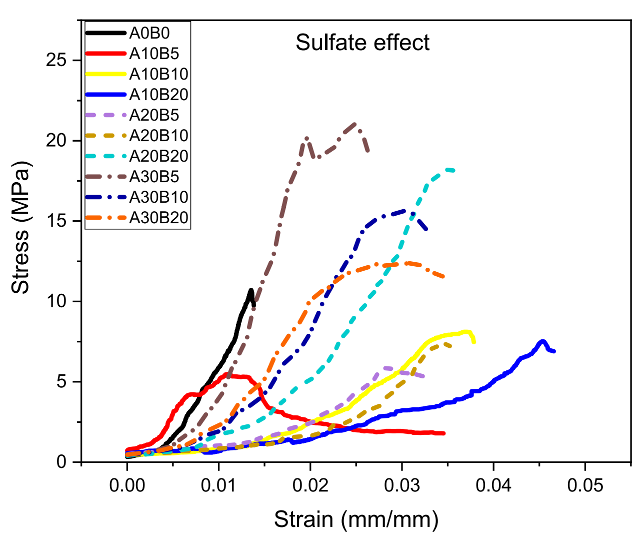

Fig. 22 Stress–strain behavior of FC mixtures after sulfate attack

3.11.3 Weight loss from exposure to sulfate attacks

The influence of BF concentration and ATP as a cement substitute on the mean weight loss of FC blends comprising 100% PA following sulfate exposure ranging from 8.79 to 12.76% is displayed in Fig. 23a. Very similar response in weight loss to the compressive strength was observed. Replacing cement with 10%ATP exhibited higher weight loss than the reference blend and the largest weight decline of 12.76% was assessed for the blend comprising 10%ATP and 0.5%BF. Cement replacement with 20%ATP showed also greater weight reduction than the reference mixture at 0.5 and 1%BF content; but the mixture 2%BF showed lower weight loss indicating that the two substances can increase the durability of FC blends to sulfate assault and effectively lower the rate of sulfate attack while producing less erosion products. Cement replacement with 30%ATP showed the lowest weight reduction at 1%BF content and other two mixtures with 0.5 and 2%BF showed also lower weight loss than most of the mixtures including the reference blend and the blends with 10, 20% ATP.

After the samples were exposed to the sulfate assault, their weight loss and compressive strength showed very significant correlation coefficient (R^2 of 0.94), indicating a parabolic connection with the increase in strength corresponding to the decrease in weight loss as illustrated in Fig. 23b.

3.11.4 Microstructure after $MgSO_4$ effect

According to Fig. 24, the A0B0 mixture's microstructure after being exposed to the $MgSO_4$ action. Ettringite crystals were seen in densely packed areas inside the matrix in SEM images. Because they expanded, these sulfate-formed crystals caused tiny fissures to appear in the matrix. Nonetheless, the impact of $MgSO_4$ caused the compressive strength to drop 1.1 times when compared to the compressive strength after 90 days.

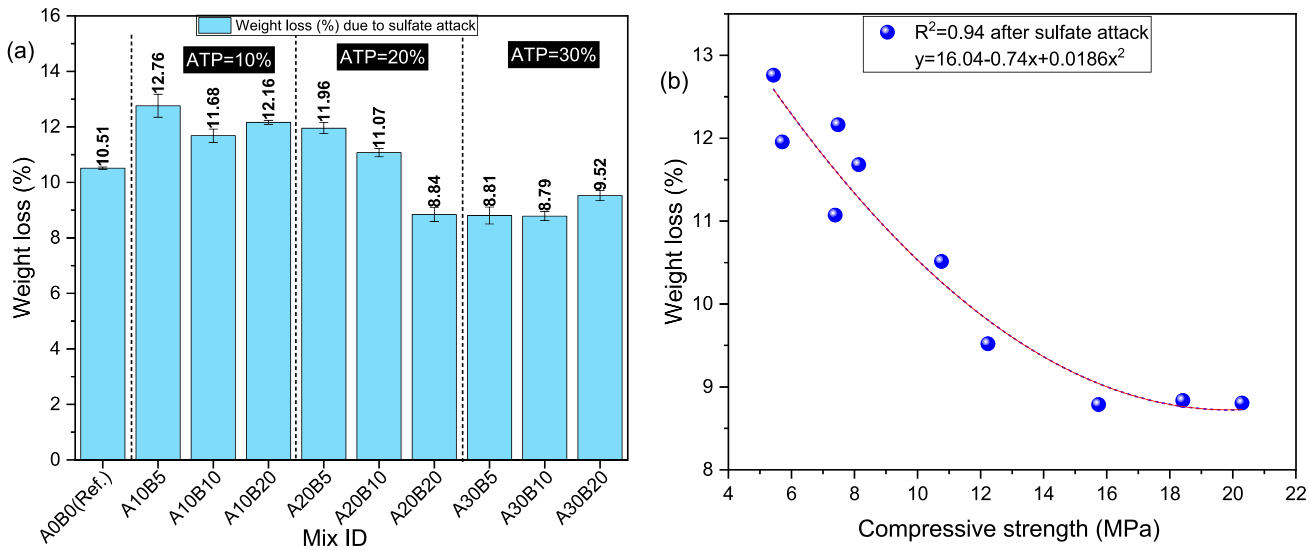

Fig. 23 **a** Weight loss and **b** compressive strength vs. weight loss of FC samples after high temperature

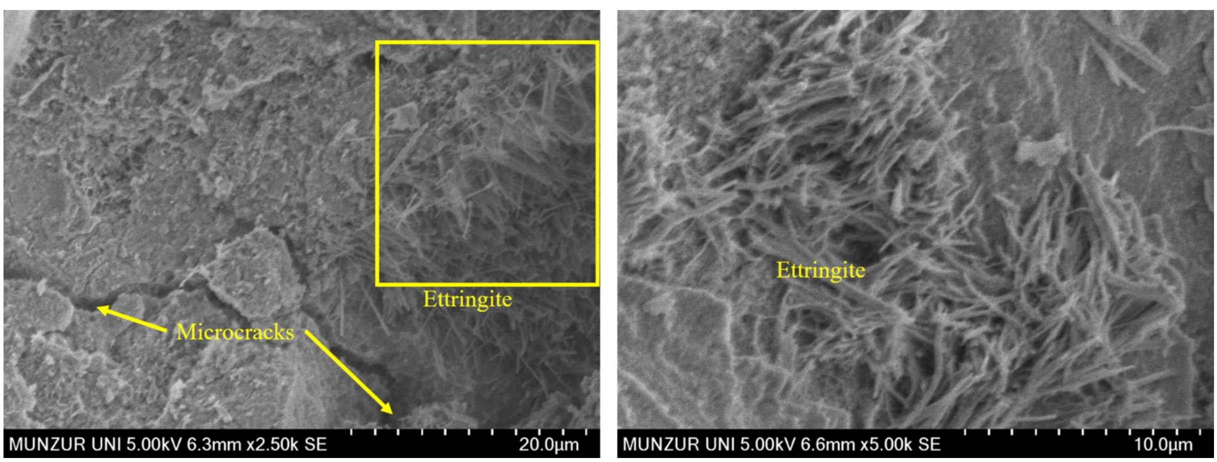

Fig. 24 Microstructure of A0B0 mixture

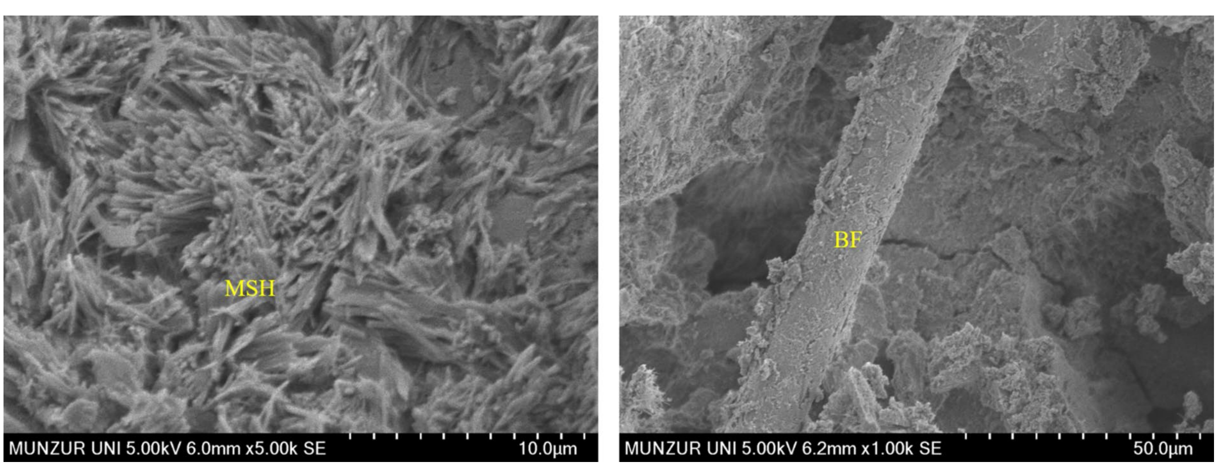

Fig. 25 Microstructure of A10B10 mixture

Figure 25 shows the microstructural changes of the A10B10 mixture. It was noted that BF was present in the matrix. Thanks to BF, micro-cracks caused by sulfa-induced expansions were significantly reduced. However, MSH structures were observed in the matrix. MSH was formed by replacing Ca in CSH. Due to this cation exchange, The A10B10 mixture's compressive strength dropped 1.5 times.

Similar results were seen in Fig. 26 for the A30B20 blend. 2% BF significantly reduced the micro-crack network in the matrix. It was observed that the pumice and BF embedded in the matrix adhered well to the matrix. Because of the impact of $MgSO_4$, the compressive strength of the A30B20 blend dropped by around 1.4 times. This decrease is again thought to be related to MSH formation. Due to the lack of frequent observations of the micro-crack network within the matrix, it was also determined that the matrix has a dense structure.

4 Conclusion

This study investigated the performance enhancements of FC modified with ATP as a partial cement substitute and BF as reinforcement, utilizing 100% pumice aggregate. By addressing the typical limitations of FC—such as low tensile strength, brittleness, and susceptibility to thermal and chemical degradation—the research aimed to develop a more robust and sustainable concrete variant suitable for demanding construction applications. Based on a comprehensive experimental program assessing mechanical, thermal, and durability properties, the following conclusions were drawn:

(a) The combined use of ATP and BF significantly improved the compressive and flexural strengths of FC. Mixtures with higher ATP content (up to 30% cement replacement) and BF inclusion showed notable increases in both strengths compared to the reference mix. The mixture containing 30% ATP and 0.5% BF achieved the highest compressive strength, demonstrating improvements of 129.3% and 85.3% at 28 and 90 days, respectively, over the control mix. This strength enhancement supports the feasibility of using this FC blend in load-bearing applications, meeting the strength requirements for structural purposes as per standard guidelines. The improvements in tensile properties due to BF inclusion addressed the inherent brittleness of FC, making it more resilient and expanding its potential for applications requiring enhanced load-bearing capacity and fracture resistance.

(b) Thermal conductivity tests indicated that the inclusion of ATP and BF affected the insulation properties of FC. The mixture with 10% ATP and 0.5% BF achieved the lowest thermal conductivity, showing a 4.2% reduction in heat transfer compared to the control mix. This reduction suggests that ATP-modified FC can provide superior insulation, making it ideal for energy-efficient buildings where thermal performance is essential. In contrast, higher ATP contents (e.g., 30%) led to increased thermal conductivity due to a denser microstructure, which, while beneficial for structural strength, was less effective for insulation.

(c) Durability assessments demonstrated that ATP and BF significantly enhanced FC's resistance to sulfate exposure and high-temperature conditions. The mixture with 30% ATP and 0.5% BF exhibited the best overall durability, showing reduced sorptivity, weight loss, and compressive strength retention even after prolonged exposure to sulfate and heating at elevated temperatures. The pozzolanic activity of ATP contributed to a denser matrix, reducing permeability and limiting the ingress of harmful ions, thus improving sulfate resistance. The presence of BF further enhanced durability by bridging micro-cracks and inhibiting crack propaga-

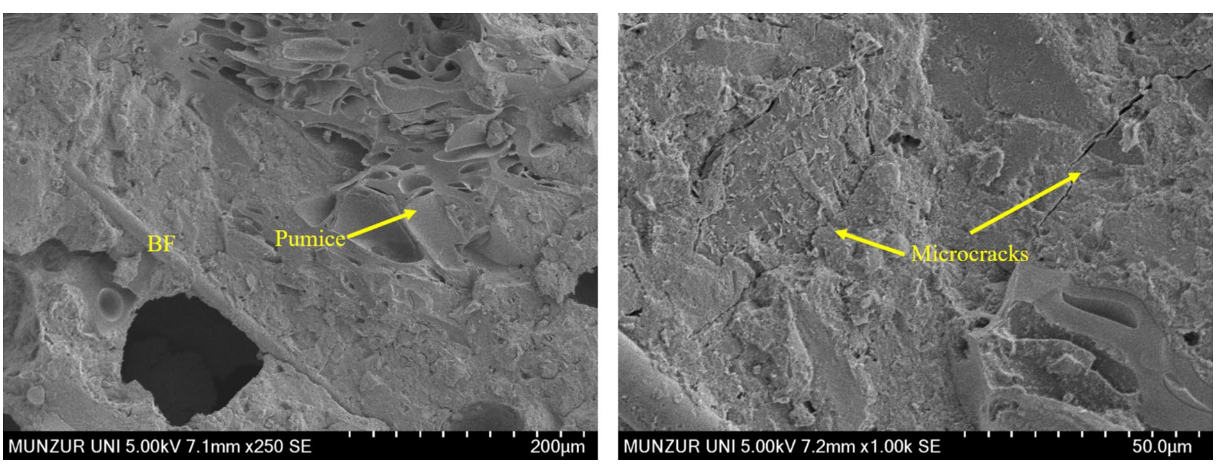

Fig. 26 Microstructure of A30B20 mixture

tion under thermal stress, particularly in mixtures with higher ATP content, such as 20% or 30%.

(d) Scanning Electron Microscopy (SEM) analysis revealed that ATP and BF induced microstructural densification and improved internal bonding within the FC matrix. ATP's pozzolanic reactivity led to the formation of additional calcium silicate hydrate (C–S–H) gel, strengthening the bond between particles and reducing porosity. BF contributed to a more interconnected and durable microstructure, with fibers acting as crack arrestors, enhancing overall cohesion and preventing the growth of micro-cracks. These microstructural changes underpinned the enhanced mechanical and durability properties observed in the experimental tests.

(e) The successful substitution of cement with up to 30% ATP, without compromising and often enhancing the mechanical and durability properties of FC, supports the study's sustainability objectives. By reducing cement content, this approach contributes to a decrease in carbon emissions associated with FC production, promoting environmentally friendly construction practices. The use of BF, which has a low environmental impact and energy-efficient production, further enhances the eco-friendliness of the proposed FC blends.

This research demonstrates that the combined use of ATP and BF in FC results in a sustainable, high-performance material that addresses key limitations of traditional foam concrete. The resulting FC variant offers improved strength, durability, and thermal properties, making it suitable for structural applications in environmentally demanding conditions, such as regions with high sulfate concentrations or thermal stress. By aligning with sustainable construction goals, these findings provide a viable pathway for the broader adoption of FC in applications where both mechanical resilience and eco-friendliness are critical. Future research could further optimize ATP and BF proportions for specific applications and investigate the long-term performance of ATP-BF-modified FC under real-world conditions.

Funding Open access funding provided by the Scientific and Technological Research Council of Türkiye (TÜBİTAK). This research received no external funding.

Data availability The data that support the findings of this study are available from the corresponding author upon reasonable request.

Declarations

Conflict of interest The author declares that he has no conflict of interest.

Ethical approval This article does not contain any studies with human participants or animals performed by any of the authors.

References

1. Amran YHM, Farzadnia N, Abang Ali AA. Properties and applications of foamed concrete; a review. Constr Build Mater. 2015;101:990–1005.
2. Raj A, Sathyan D, Mini KM. Physical and functional characteristics of foam concrete: a review. Constr Build Mater. 2019;221:787–99.
3. Bayraktar OY, Kaplan G, Gencel O, Benli A, Sutcu M. Physico-mechanical, durability and thermal properties of basalt fiber reinforced foamed concrete containing waste marble powder and slag. Constr Build Mater. 2021;288: 123128.
4. Gencel O, Nodehi M, Bayraktar OY, Kaplan G, Benli A, Gholampour A, Ozbakkaloglu T. Basalt fiber-reinforced foam concrete containing silica fume: an experimental study. Constr Build Mater. 2022;326: 126861.
5. Gencel O, Benli A, Bayraktar OY, Kaplan G, Sutcu M, Elabade WAT. Effect of waste marble powder and rice husk ash on the microstructural, physico-mechanical and transport properties of foam concretes exposed to high temperatures and freeze-thaw cycles. Constr Build Mater. 2021;291: 123374.
6. Gencel O, Bayraktar OY, Kaplan G, Benli A, Martinez-Barrera G, Brostow W, Tek M, Bodur B. Characteristics of hemp fibre reinforced foam concretes with fly ash and Taguchi optimization. Constr Build Mater. 2021;294: 123607.
7. Gencel O, Bayraktar OY, Kaplan G, Arslan O, Nodehi M, Benli A, Gholampour A, Ozbakkaloglu T. Lightweight foam concrete containing expanded perlite and glass sand: physico-mechanical, durability, and insulation properties. Constr Build Mater. 2022;320: 126187.
8. Gencel O, Balci B, Bayraktar OY, Nodehi M, Sari A, Kaplan G, Hekimog G, Gholampour A, Benli A, Ozbakkaloglu T. The effect of limestone and bottom ash sand with recycled fine aggregate in foam concrete. J Build Eng. 2022;54: 104689.
9. Bayraktar OY, Yarar G, Benli A, Kaplan G, Gencel O, Sutcu M, Kozlowski M, Kadela M. Basalt fiber reinforced foam concrete with marble waste and calcium aluminate cement. Struct Concr. 2023;24(1):1152–78.
10. Özkan IGM, Aldemir K, Alhasan O, Benli A, Bayraktar OY, Yilmazoglu MU, Kaplan G. Investigation on the sustainable use of different sizes of sawdust aggregates in eco-friendly foam concretes: Physico-mechanical, thermal insulation and durability characteristics. Constr Build Mater. 2024;438: 137100.
11. Bayraktar OY, Tunçtan M, Benli A, Türkel I, Kizilay G, Kaplan G. A study on sustainable foam concrete with waste polyester and ceramic powder: properties and durability. J Build Eng. 2024;95: 110253.

12. Sahu SS, Gandhi ISR. Studies on influence of characteristics of surfactant and foam on foam concrete behavior. J Build Eng. 2021;40: 102333.
13. Gao HY, Wang WG, Liao HQ, Cheng FQ. Characterization of light foamed concrete containing fly ash and desulfurization gypsum for wall insulation prepared with vacuum foaming process. Constr Build Mater. 2021;281: 122411.
14. Benli A. Sustainable use of waste glass sand and waste glass powder in alkali-activated slag foam concretes: physico-mechanical, thermal insulation and durability characteristics. Constr Build Mater. 2024;438: 137128.
15. Li MG, Tan HB, He XY, Jian SW, Li GY, Zhang JJ, Deng XF, Lin XL. Enhancement in compressive strength of foamed concrete by ultra-fine slag. Cem Concr Comp. 2023;138: 104954.
16. Alqarni AS. A comprehensive review on properties of sustainable concrete using volcanic pumice powder ash as a supplementary cementitious material. Constr Build Mater. 2022;323: 126533.
17. Tanyildizi M, Gökalp I. Utilization of pumice as aggregate in the concrete: a state of art. Constr Build Mater. 2023;377: 131102.
18. Jamal AS, Bzeni DKH, Shi JY. Thermal and mechanical performance of lightweight geopolymer concrete with pumice aggregate. Struct Concr. 2024;25(1):349–64.
19. Dener M, Karatas M, Mohabbi M. Sulfate resistance of alkali-activated slag/portland cement mortar produced with lightweight pumice aggregate. Constr Build Mater. 2021;304: 124671.
20. Karatas M, Balunb B, Benli A. High temperature resistance of self-compacting lightweight mortar incorporating expanded perlite and pumice. Comput Concr. 2017;19(2):121–6.
21. Gündüz L, Ugur I. The effects of different fine and coarse pumice aggregate/cement ratios on the structural concrete properties without using any admixtures. Cem Concr Res. 2005;35(9):1859–64.
22. Bodur B, Isik MAM, Benli A, Bayrak B, Öz A, Bayraktar OY, Kaplan G, Aydin AC. Durability of green rubberized 3D printed lightweight cement composites reinforced with micro attapulgite and micro steel fibers: printability and environmental perspective. J Build Eng. 2024;90: 109447.
23. Gencel O, Ustaoglu A, Benli A, Hekimoglu G, Sari A, Erdogmus E, Sutcu M, Kaplan G, Bayraktar OY. Investigation of physico-mechanical, thermal properties and solar thermoregulation performance of shape-stable attapulgite based composite phase change material in foam concrete. Sol Energy. 2022;236:51–62.
24. Zghair LAG, Hamad HH, Mohamad SA, Al-Hamd RKS. Evaluate the compressive strength of cement paste modified with high reactivity attapulgite and affected by curing temperature. Mater Today Proc. 2021;52:361–6.
25. Kawashima S, Chaouche M, Corr DJ, Shah SP. Influence of purified attapulgite clays on the adhesive properties of cement pastes as measured by the tack test. Cem Concr Compos. 2014;48:35–41.
26. Manharawy MS, Mahmoud AA, El-Mahdy OO, El-Diasity MH. Experimental and numerical investigation of lightweight foamed reinforced concrete deep beams with steel fibers. Eng Struct. 2022;260: 114202.
27. Falliano D, De Domenico D, Ricciardi G, Gugliandolo E. Compressive and flexural strength of fiber-reinforced foamed concrete: effect of fiber content, curing conditions and dry density. Constr Build Mater. 2019;198:479–93.
28. Shi XX, Ning BK, Liu JP, Wei ZS. Effects of re-dispersible latex powder-basalt fibers on the properties and pore structure of lightweight foamed concrete. J Build Eng. 2023;75: 106984.
29. Mydin MAO, Nawi MNM, Omar R, Dulaimi A, Najm HM, Mahmood S, Sabri MMS. Mechanical, durability and thermal properties of foamed concrete reinforced with synthetic twisted bundle macro-fibers. Front Mater. 2023;10:1158675.
30. Adesina A. Performance of cementitious composites reinforced with chopped basalt fibres—an overview. Constr Build Mater. 2021;266: 120970.
31. Sim J, Park C, Moon DY. Characteristics of basalt fiber as a strengthening material for concrete structures. Compos Part B Eng. 2005;36(6–7):504–12.
32. Branston J, Das S, Kenno SY, Taylor C. Influence of basalt fibres on free and restrained plastic shrinkage. Cem Concr Comp. 2016;74:182–90.
33. Wang XQ, Jin YL, Huang W, Li X, Ma Q. Effect of hybrid basalt and sisal fibers on durability and mechanical properties of lightweight roadbed foam concrete. Case Stud Constr Mater. 2023;19:e02592.
34. ASTM C33-16, Standard specification for concrete aggregates. ASTM Int. 2016. https://doi.org/10.1520/C0033_C0033M-16.
35. ASTM, ASTM C1437-15 Standard test method for flow of hydraulic cement mortar. West Conshohocken: ASTM International; 2015.
36. ASTM C642-13 Standard test method for density, absorption, and voids in hardened concrete. West Conshohocken: ASTM International; 2013.
37. ASTM, ASTM C348-19 standard test method for flexural strength of hydraulic-cement mortars. West Conshohocken: ASTM International; 2019.
38. ASTM, ASTM C349-18 standard test method for compressive strength of hydraulic-cement mortars (using portions of prisms broken in flexure). West Conshohocken: ASTM International; 2018.
39. ASTM C469, "Standard test method for static modulus of elasticity and Poisson's ratio of concrete in compression," Annual Book of ASTM Standard; 2010.
40. ASTM C518-21 Standard test method for steady-state thermal transmission properties by means of the heat flow meter apparatus. West Conshohocken: ASTM International; 2021.
41. ASTM, ASTM C1585-20 Standard test method for measurement of rate of absorption of water by hydraulic-cement concretes. West Conshohocken: ASTM International; 2020.
42. ASTM, ASTM C1012/C1012M-18b Standard test method for length change of hydraulic-cement mortars exposed to a sulfate solution. West Conshohocken: ASTM International; 2018.
43. Bodian M, Keinde D, Yade I, Hannawi K, Agbodjan PW, Fall M, Darquennes A. Study of attapulgite as an additive in reinforced concrete by substitution of cement and its effects on the durability properties of hardened concrete. Open J Civ Eng. 2022;12(3):301–19.
44. Saeed IA, Mohammed TJ, Jihad SAA. Partial replacement of sand with attapulgite in concrete. Int Rev Civ Eng. 2020;11(2):73.
45. Shi JB, Li M. Surface modification effects in phase change material-infiltrated attapulgite. Mater Chem Phys. 2020;254: 123521.
46. Song SK, Dong LJ, Chen S, Xie HA, Xiong CX. Stearic-capric acid eutectic/activated-attapulgiate composite as form-stable phase change material for thermal energy storage. Energy Convers Manag. 2014;81:306–11.
47. Bayraktar OY, Kaplan G, Shi JY, Benli A, Bodur B, Turkoglu M. The effect of steel fiber aspect-ratio and content on the fresh, flexural, and mechanical performance of concrete made with recycled fine aggregate. Constr Build Mater. 2023;368: 130497.
48. Benli A, Bayraktar OY, Koksal F, Kaplan G. Sustainable use of recycled fine aggregates in steel fiber-reinforced concrete: fresh, flexural, mechanical and durability characteristics. J Build Eng. 2024;97:110745.
49. Wang YG, Li SP, Hughes P, Fan YH. Mechanical properties and microstructure of basalt fibre and nano-silica reinforced recycled concrete after exposure to elevated temperatures. Constr Build Mater. 2020;247:118561.

50. Koksal F, Yildirim MS, Benli A, Gencel O. Hybrid effect of micro-steel and basalt fibers on physico-mechanical properties and durability of mortars with silica fume. Case Stud Constr Mater. 2021;15:e00649.
51. Koksal F, Kocabeyoglu ET, Gencel O, Benli A. The effects of high temperature and cooling regimes on the mechanical and durability properties of basalt fiber reinforced mortars with silica fume. Cem Concr Comp. 2021;121: 104107.
52. Niaki MH, Fereidoon A, Ahangari MG. Experimental study on the mechanical and thermal properties of basalt fiber and nanoclay reinforced polymer concrete. Compos Struct. 2018;191:231–8.
53. ACI 318-14, Building Code Requirements for Structural Concrete. 2014.
54. Liu Y, Han J, Li M, Yan P. Effect of a nanoscale viscosity modifier on rheological properties of cement pastes and mechanical properties of mortars. Constr Build Mater. 2018;190:255–64.
55. Langaroudi MAM, Mohammadi Y. Effect of nano-clay on workability, mechanical, and durability properties of self-consolidating concrete containing mineral admixtures. Constr Build Mater. 2018;191:619–34.
56. Kawashima S, Chaouche M, Corr DJ, Shah SP. Rate of thixotropic rebuilding of cement pastes modified with highly purified attapulgite clays. Cem Concr Res. 2013;53:112–8.
57. Kaplan G, Bayraktar OY, Memis S. Effect of high volume fly ash and micro-steel fiber on flexural toughness and durability properties in self-compacting lightweight mortar (SCLM). Constr Build Mater. 2021;307: 124877.
58. Khan M, Cao ML, Ali M. Effect of basalt fibers on mechanical properties of calcium carbonate whisker-steel fiber reinforced concrete. Constr Build Mater. 2018;192:742–53.
59. Koksal F, Bacanli C, Benli A, Gencel O. Fresh, flexural and mechanical performance of polyamide and polypropylene based macro-synthetic fiber-reinforced concretes. Struct Eng Mech. 2022;82(1):93–105.
60. ASTM C330/C330M-17. Standard Specification for Lightweight Aggregates for Structural Concrete; ASTM C330/C330M-17a. West Conshohocken: ASTM International; 2017.
61. Kearsley EP, Wainwright PJ. The effect of porosity on the strength of foamed concrete. Cem Concr Res. 2002;32(2):233–9.
62. Li J, Xia J, Di Sarno L, Gong G. Fiber utilization in pervious concrete: Review on manufacture and properties. Constr Build Mater. 2023;406: 133372.
63. Lindgreen H, Geiker M, Krøyer H, Springer N, Skibsted J. Microstructure engineering of Portland cement pastes and mortars through addition of ultrafine layer silicates. Cem Concr Compos. 2008;30(8):686–99.
64. Benli A, Karatas M, Bakir Y. An experimental study of different curing regimes on the mechanical properties and sorptivity of self-compacting mortars with fly ash and silica fume. Constr Build Mater. 2017;144:552–62.
65. Kaplan G, Coskan U, Benli A, Bayraktar OY, Kucukbaltaci AB. The impact of natural and calcined zeolites on the mechanical and durability characteristics of glass fiber reinforced cement composites. Constr Build Mater. 2021;311:125336.
66. Turkoglu M, Bayraktar OY, Benli A, Kaplan G. Effect of cement clinker type, curing regime and activator dosage on the performance of one-part alkali-activated hybrid slag/clinker composites. J Build Eng. 2023;68:106164.
67. Bing C, Liu JY. Residual strength of hybrid-fiber-reinforced high-strength concrete after exposure to high temperatures. Cem Concr Res. 2004;34(6):1065–9.
68. Shi T, Liu Y, Zhang Y, Lan Y, Zhao Q, Zhao Y, Wang H. Calcined attapulgite clay as supplementary cementing material: thermal treatment, hydration activity and mechanical properties. Int J Concr Struct Mater. 2022;16(1):1–10.
69. Yildirim M, Özhan HB. Durability properties of basalt fiber-reinforced mortars with different mineral admixtures exposed to high temperatures. Constr Build Mater. 2023;400: 132574.
70. Chen XD, Shi DD, Zhang JH, Cheng XY. Experimental investigation of the residual physical and mechanical properties of foamed concrete exposed to high temperatures. J Mater Civ Eng. 2021;33(7):3779.
71. Bayraktar OY, Eshtewi SST, Benli A, Kaplan G, Toklu K, Gunek F. The impact of RCA and fly ash on the mechanical and durability properties of polypropylene fibre-reinforced concrete exposed to freeze-thaw cycles and $MgSO_4$ with ANN modeling. Constr Build Mater. 2021;313:125508.
72. Kaplan G, Bayraktar OY, Bayrak B, Celebi O, Bodur B, Oz A, Aydin AC. Physico-mechanical, thermal insulation and resistance characteristics of diatomite and attapulgite based geopolymer foam concrete: effect of different curing regimes. Constr Build Mater. 2023;373: 130850.